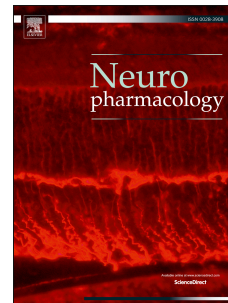


# Accepted Manuscript

Protons modulate gating of recombinant  $\alpha_1\beta_2\gamma_2$  GABA<sub>A</sub> receptor by affecting desensitization and opening transitions

Magdalena Kisiel, Magdalena Jatczak-Śliwa, Jerzy W. Mozrzymas



PII: S0028-3908(18)30800-1

DOI: [10.1016/j.neuropharm.2018.10.016](https://doi.org/10.1016/j.neuropharm.2018.10.016)

Reference: NP 7387

To appear in: *Neuropharmacology*

Received Date: 6 March 2018

Revised Date: 28 September 2018

Accepted Date: 12 October 2018

Please cite this article as: Kisiel, M., Jatczak-Śliwa, M., Mozrzymas, J.W., Protons modulate gating of recombinant  $\alpha_1\beta_2\gamma_2$  GABA<sub>A</sub> receptor by affecting desensitization and opening transitions, *Neuropharmacology* (2018), doi: <https://doi.org/10.1016/j.neuropharm.2018.10.016>.

This is a PDF file of an unedited manuscript that has been accepted for publication. As a service to our customers we are providing this early version of the manuscript. The manuscript will undergo copyediting, typesetting, and review of the resulting proof before it is published in its final form. Please note that during the production process errors may be discovered which could affect the content, and all legal disclaimers that apply to the journal pertain.

**Title**

Protons modulate gating of recombinant  $\alpha_1\beta_2\gamma_2$  GABA<sub>A</sub> receptor by affecting desensitization and opening transitions

**Author names and affiliations**

Magdalena Kisiel<sup>1</sup>, Magdalena Jatczak-Śliwa<sup>1,2</sup>, Jerzy W Mozrzymas<sup>1</sup>

1 Laboratory of Neuroscience, Department of Biophysics, Wrocław Medical University, Wrocław 50-368, Poland

2 Department of Molecular Physiology and Neurobiology, Wrocław University, Wrocław 50-335, Poland

**Corresponding author**

Correspondence should be addressed to either of the following: Magdalena Kisiel, Laboratory of Neuroscience, Department of Biophysics, Wrocław Medical University, ul. Chałubińskiego 3, Wrocław, 50-368, Poland. E-mail: [kisiel.magda@gmail.com](mailto:kisiel.magda@gmail.com); or Jerzy W. Mozrzymas, Laboratory of Neuroscience, Department of Biophysics, Wrocław Medical University, ul. Chałubińskiego 3, Wrocław, 50-368, Poland. E-mail: [jerzy.mozrzymas@umed.wroc.pl](mailto:jerzy.mozrzymas@umed.wroc.pl)

**Authorship contribution statement**

JWM conceived the project, obtained financial support and supervised project realisation, participated in designing and performing of experiments and in model simulations.

MK participated in designing of experiments, performed model simulations, most of experiments and gross of data analysis.

MJ-Ś participated in performing of experiments and in data analysis.

All authors wrote the paper.

**Keywords**

$\gamma$ -aminobutyric acid; gating; macroscopic currents; single-channel recordings; extracellular pH

**Abbreviations**

A<sub>fast</sub>, percentage of fast component of deactivation; A<sub>slow</sub>, percentage of slow component of deactivation; ATP, adenosine 5'-triphosphate; CD4, cluster of differentiation 4; cDNA, complementary deoxyribonucleic acid; CYS,  $\alpha_1$ Phe64Cys $\beta_2\gamma_2$  mutant(s); EGTA, egtazic acid, ethylene glycol-bis(2-aminoethylether)-N,N,N',N'-tetraacetic acid; fJWm, flipped Jones-Westbrook's model; FR10, fraction remaining after 10 ms from peak; GABA<sub>A</sub>R(s), GABA type A receptor(s); HEK, Human Embryonic Kidney cell line; HEPES, buffer 2-[4-(2-hydroxyethyl)piperazin-1-yl]ethanesulfonic acid; LEU,  $\alpha_1$ Phe64Leu $\beta_2\gamma_2$  mutant(s); MES, 4-morpholineethanesulfonic acid, 2-(N-morpholino)ethanesulfonic acid hydrate; P<sub>i</sub> (P<sub>1</sub>%), area (percentage) of specific (i<sup>th</sup>) open or shut time component; P4S, piperidine-4-sulphonic acid; pCMV, vector with cytomegalovirus promoter; pH, potential of hydrogen, the negative (of the base 10) logarithm of the molar concentration of protons; P<sub>OpenMax</sub>, maximum open probability; ss/peak, steady-state amplitude to peak amplitude ratio; t<sub>crit</sub>, critical time;  $\tau_{deact}$ , mean deactivation time; TEA-Cl, tetraethylammonium chloride;  $\tau_{fast}$ , time constant of fast component of deactivation;  $\tau_{fastDes}$ , time constant of fast component of macroscopic desensitization;  $\tau_{open}$ , mean open time;  $\tau_{slow}$ , time constant of slow component of deactivation; WT, wild-type  $\alpha_1\beta_2\gamma_2$  receptor(s)

## Abstract

Protons are potent modulators of GABA<sub>A</sub> receptors (GABA<sub>A</sub>Rs) and  $\alpha_1$ Phe64 residue was implicated in their pH sensitivity. Recently, we have demonstrated that this residue is involved in flipping transitions which precede channel opening. We thus re-addressed the mechanism of GABA<sub>A</sub>R modulation by protons by considering the gating scheme extended by flipping. The impact of pH changes was examined on currents mediated by wild-type  $\alpha_1\beta_2\gamma_2$  receptors or by their  $\alpha_1$ Phe64Leu or  $\alpha_1$ Phe64Cys mutants and elicited by saturating concentrations of full (GABA) or partial (piperidine-4-sulfonic acid) agonists. To describe the impact of extracellular pH on receptor gating, we combined macroscopic analysis of currents elicited by rapid agonist applications with single-channel studies. Acidification (pH 6.0) increased current amplitudes (in the case of leucine mutants effect was stronger when P4S was used) and decreased the rate and the extent of desensitization whereas alkalization (pH 8.0) had the opposite but weaker effect. Deactivation kinetics for wild-type receptors was slowed down by acidification while in the case of mutants this effect was observed upon alkalization. Moreover,  $\alpha_1$ Phe64 mutations enhanced GABA<sub>A</sub>R sensitivity to alkaline pH. Single-channel analysis revealed that acidification prolonged burst durations and affected shut but not open time distributions. Model simulations for macroscopic and single-channel activity indicated a novel mechanism in which protons primarily affected opening and desensitization rates but not flipping/unflipping. This evidence for the impact of protons on the receptor gating together with previously demonstrated effect on the agonist binding, point to a complex effect of extracellular pH on GABA<sub>A</sub>R macromolecule.

## 1. Introduction

GABA<sub>A</sub> receptors are ionotropic channels and play a crucial role in mediating inhibitory neurotransmission in adult mammalian CNS (Brickley and Mody, 2012; Farrant and Nusser, 2005; Sieghart, 2006). pH level is regulated by various mechanisms – e.g. by carbonic anhydrase, co-transporters or active and passive transport (Kaila, 1994). Typically, neuronal activity induces relatively small pH changes - about 0.2 in pH units (Chen and Chesler, 1992, 1991; Kaila, 1994). However, local pH changes in the closest vicinity of GABAergic synapse can be larger due to permeation of HCO<sub>3</sub><sup>-</sup> anions by GABA<sub>A</sub>Rs resulting in alkalization of extracellular medium (Kaila and Voipio, 1987). On the other hand, dumping of highly acidic vesicle content into synaptic cleft upon agonist release may transiently reduce local pH level (DeVries, 2001; Miesenböck et al., 1998; Palmer et al., 2003). Moreover, Dietrich and Morad (2010) provided evidence that Na<sup>+</sup>/H<sup>+</sup> exchanger contributes to synaptic acidification. It needs to be also emphasized that in pathological conditions such as ischemia, hypothermia or inflammation, large changes of pH level (about 1 pH unit) toward acidosis can be observed (Hoffman et al., 1999, 1996; Kraig et al., 1987). Thus, several mechanisms may be involved in regulation of extracellular pH in the vicinity of GABAergic synapses giving rise to potentially large changes in proton concentration. It is known that GABA<sub>A</sub>Rs can be strongly modulated by extracellular concentration of protons (Chen and Huang, 2014; Feng and Macdonald, 2004; Huang and Dillon, 1999; Krishek and Smart, 2001; Krishek et al., 1996; Pasternack et al., 1996; Robello et al., 1994). Our previous papers related to this subject (Mercik et al., 2006; Mozrzymas et al., 2003b; Wójtowicz et al., 2008) suggested that the mechanism of this modulation involves binding and desensitization processes. However, previous investigations related to the mechanisms of GABA<sub>A</sub>Rs by protons were based on simplified gating models. Indeed, recent studies (Dixon et al., 2015; Gielen et al., 2012; Kisiel et al., 2018; Szczot et al., 2014) provided evidence that GABA<sub>A</sub>R gating scheme needs to be upgraded by so called flipping transition upon which channel remains closed but its propensity to opening is enhanced. The concept of flipping transitions has been consistently reported also for other members of Cys-loop receptors family (Burzomato et al., 2004; Corradi and Bouzat, 2014; Jadey and Auerbach, 2012; Lape et al., 2008; Mukhtasimova et al., 2009). Emerging multiplicity of gating transitions in the GABA<sub>A</sub>Rs kinetic scheme (Kisiel et al., 2018) points to the need to extend the approach based on investigations of non-equilibrium macroscopic currents by single-channel analysis (Colquhoun and Lape, 2012) which turns out to be particularly reliable and informative when studying complex mechanisms. Interestingly, (Huang et al., 2004) reported that the  $\alpha_1$ Phe64 residue (loop D, part of GABA-binding site) is involved in GABA<sub>A</sub>R sensitivity to pH whereas our study (Szczot et al., 2014) provided evidence that mutation of this residue strongly affects not only agonist binding but also the flipping transition. This raises the possibility that the impact of protons on GABA<sub>A</sub>Rs can be related to modulation of flipping transitions. However, our more recent study based on single-channel analysis (Kisiel et al., 2018) has demonstrated that the  $\alpha_1$ Phe64 residue is involved not only in flipping but also in later gating transitions – openings and closings. Considering that mutations of the  $\alpha_1$ Phe64 residue differentially affect specific gating properties, we found it appealing to study the impact of protons on different mutants at this residue. These premises point to the need of a comprehensive approach, enabling us to extract reliable information on how changes in extracellular pH affect specific gating transitions of the GABA<sub>A</sub> receptor. We addressed this issue by analysing macroscopic and single-channel currents mediated by wild-type (WT) and mutated ( $\alpha_1$ Phe64Cys/Leu)  $\alpha_1\beta_2\gamma_2$  receptors and evoked by saturating concentration of full or partial agonist. Our results indicate that the mechanism of pH modulation involves alteration of desensitization and opening/closing transitions but flipping appears not to be affected. The impact of mutation at

the binding site residue ( $\alpha_1$ Phe64) on modulation of GABA<sub>A</sub>R gating by protons further confirms that this residue affects very distant structures of this macromolecule altering thereby late phases of the receptor gating.

## 2. Material and methods

### 2. 1. Cell Culture and Transfection

The receptors were expressed in HEK293 cell line (Human Embryonic Kidney). Cells were transfected using calcium phosphate precipitation method (Chen and Okayama, 1987). cDNA encoding rat GABA<sub>A</sub>R subunits and human CD4 (cloned in pCMV vectors) were added in the following proportions  $\alpha_1:\beta_2:\gamma_{2L}:CD4$  – 1:1:3:1 ( $\mu$ g) in 1 ml of transfection solution. To detect transfected cells, CD4 beads (Dynabeads, Life Technologies) were used. In the cases of excessive channel expression (predominance of overlapping single-channel events in patch-clamp recordings) empty plasmid was used and amounts of other plasmids were decreased accordingly (total amount of cDNA plasmid was 4  $\mu$ g). The plasmid encoding the  $\alpha_1$ Phe64Leu subunit was kindly given by Dr. Erwin Siegel,  $\alpha_1$ Phe64Cys – by Dr. Andrea Barberis and empty plasmids – by Dr. Lucia Sivilotti.

### 2. 2. Electrophysiological Recordings

Recordings were performed in voltage-clamp configuration of the patch-clamp technique, using the Axopatch 200B amplifier. Signals were digitized using a Digidata 1440 card. For acquisition and analysis, pClamp 10 software was used. Recording/acquisition devices and software were from Molecular Devices.

Macroscopic currents were recorded in the whole-cell (lifted cell) or outside-out configurations at a holding potential of -40 mV. Signals were low-pass filtered at 10 kHz and sampled at 100 kHz. Agonists were applied using the ultrafast perfusion system based on piezoelectric-driven (Physics Instrumente) theta-glass pipettes (Hilgenberg; Jonas, 1995). The onset of the open-tip junctional potential was 100-300  $\mu$ s. The resistance of patch pipettes filled with intrapipette solution was 3-6 M $\Omega$ . The internal solution consisted of (in mM): 137 KCl, 11 EGTA, 10 K-gluconate, 10 HEPES, 2 MgCl<sub>2</sub>, 2 ATP, 1 CaCl<sub>2</sub>, pH was set to 7.2 with KOH. External saline contained (in mM): 137 NaCl, 20 glucose, 10 HEPES, 5 KCl, 2 CaCl<sub>2</sub>, 1 MgCl<sub>2</sub>, with pH adjusted with NaOH. HEPES was used to buffer solutions with pH 7.2 and 8.0, 15 mM MES for pH 6.0. To maintain the osmolarity at a constant level, for GABA concentrations higher than 10 mM, NaCl/KCl concentrations were reduced to 87 mM and wash solutions were supplemented with glucose and the internal solution with 50 mM K-gluconate (Szczot et al., 2014; Wagner et al., 2004). Access resistance was controlled and its typical value was below 10 M $\Omega$ . The impact of compensation was negligible for currents not exceeding 2 nA and only such responses were included in the analysis. For amplitude comparisons only stable recordings were included in which run-down or run-up did not exceed 25% of current initial amplitude. To assess the impact of pH changes, for each recording at any considered pH, control currents (pH 7.2) were measured before and after the test recording (at equal time distances). This procedure was applied to monitor the extent of rundown and to correct it by interpolating the control value at the time of the test recording. This means that for each test recording an “individual” control value was determined (interpolated from two control recordings). This procedure allowed us to correct for the rundown and to apply the paired tests to assess the significance between control and test groups. The macroscopic currents were recorded for wild type  $\alpha_1\beta_2\gamma_2$  receptors (WT) or for leucine (LEU) or cysteine (CYS) mutants at  $\alpha_1$ Phe64 residue.  $\gamma$ -aminobutyric acid (GABA) or piperidine-4-sulfonic acid (P4S) were used as standard and partial agonists, respectively.

Respective groups of recordings were named according to the receptor type and the agonist used, e.g. WT-GABA or LEU-P4S.

Single-channel recordings for the wild-type GABA<sub>A</sub> receptors were performed in the cell-attached configuration for currents evoked by saturating [GABA]. To assure the consistency with our recent investigations, extensive single-channel data obtained at pH 7.4 presented in (Kisiel et al., 2018), were used as controls and compared to those recorded at pH 6.0. The intrapipette solution had the same composition as the external one but also contained the agonist and consisted of (in the case of solutions with 10 mM GABA) in mM: 102.7 NaCl, 20 Na-gluconate, 2 CaCl<sub>2</sub>, 2 KCl, 1.2 MgCl<sub>2</sub>, 10 HEPES, 20 TEA-Cl, 14 D(+)-glucose, 15 Sucrose, with pH adjusted to 7.4 by 2 M NaOH. A low-chloride solution used in experiments with 30 mM GABA contained in mM: 70 NaCl, 10 Na-gluconate, 2 CaCl<sub>2</sub>, 2 KCl, 1.2 MgCl<sub>2</sub>, 10 HEPES, 20 TEA-Cl and D(+)-glucose (in the amount needed to obtain similar osmolarity as for 10 mM GABA). Pipette electrodes were pulled from borosilicate glass capillaries (Hilgenberg), coated with Sylgard 184 (Dow Corning), and fire-polished to 6-10 MΩ (with the internal solution). Single-channel currents were low-pass filtered at 10 kHz, and sampled at 100 kHz. Typically, recordings were performed at different holding voltages (-50 to +100 mV for conductance assessment and +100 mV for kinetic analysis) as free run sweeps lasting for a few minutes.

All chemicals were from Sigma Aldrich. Experiments were carried out at room temperature.

### 3. Theory/calculation

#### 3.1. Macroscopic currents

The onset kinetics of current responses was assessed as 10-90% Rise Time or by fitting with an exponential function:

$$I(t) = A_{peak} \cdot (1 - e^{-\frac{t}{\tau}}) \quad \text{Eq. 1}$$

$A_{peak}$  - the current amplitude,  $\tau$  - the time constant. Then, the 10-90% Rise Time was calculated as  $\tau \cdot \ln 9$ . Kinetics of current deactivation was fitted with a sum of exponential functions.

$$I(t) = \sum_{i=1}^n A_i \cdot e^{-\frac{t}{\tau_i}} \quad \text{Eq. 2}$$

$A_i$  is the amplitude,  $\tau_i$  - the time constant (e.g.  $\tau_{slow}$ ,  $\tau_{fast}$ ),  $n$  - the number of components. The deactivation mean time was calculated using the equation:  $\tau_{deact} = \sum_{i=1}^n a_i \tau_i$ , where  $a_i$  - the normalized weight of a particular amplitude component calculated as  $a_i = A_i \cdot (\sum_{i=1}^n A_n)^{-1}$ . The fast component of macroscopic desensitization observed upon prolonged application of saturating agonist concentration was described by fitting with a single exponential function to the trace within a limited time window (typically 30-50 ms):

$$I(t) = A_{fast} \cdot e^{-\frac{t}{\tau_{fastDes}}} + C \quad \text{Eq. 3}$$

$A_{fast}$  is the current amplitude of the fast component,  $\tau_{fastDes}$  - the time constant of fast desensitization, and  $C$  - the constant value representing the non-desensitizing current. The fraction of this current can be assessed as  $C/(A+C)$  or as the *ss/peak* parameter. In the case of mutated receptors or responses to partial agonist applications, for which desensitization kinetics was too slow for exponential fitting, the extent of desensitization was evaluated as the

*FR10* parameter defined as a fraction of current remaining after 10 ms from the peak relative to the peak.

### 3. 2. Non-stationary variance analysis

Although single-channel conductance could be directly measured in our single-channel analysis (see below), we have employed non-stationary variance analysis (NSVA) for currents elicited by rapid agonist applications to assess the maximum open probability ( $P_{openMax}$ ) in the dynamic conditions. This was considered important because direct comparison of kinetic features of receptors in dynamic conditions (jumps) and in the steady-state conditions (single-channel recordings) revealed substantial differences (see chapters 4.1 in Results and 5.2 in Discussion). NSVA was performed on currents (at least 10 responses to short application of saturating agonist concentrations) measured from the same patch. For this analysis, the custom MatLab script (Mathworks) was used. Current amplitudes ( $A$ ) and noise variances ( $\sigma^2$ ) were estimated for each time point from peak to baseline (De Koninck and Mody, 1994). The values of current amplitude were divided into 100 equal bins and the corresponding variances were averaged. Plots of variance versus current were fitted with the equation:

$$\sigma^2 = iA - \frac{A^2}{N} + c \quad \text{Eq. 4}$$

where  $i$  is the single-channel current,  $N$  - the number of channels and  $c$  - the baseline noise (Ghavanini et al., 2006). The maximum open probability ( $P_{OpenMax}$ ) was calculated as:  $P_{OpenMax} = A_{peak} \cdot (i \cdot N)^{-1}$ .

### 3. 3. Single-channel analysis

Single-channel kinetic analysis was carried out using SCAN and EKDIST software (kindly given to our group by David Colquhoun, DCWinprogs). Single-channel traces selected for analysis had at least 10000 events of cluster activity evoked by saturating [GABA]. Recorded traces (stored in the form of \*.abf - Axon Binary File) were filtered to get the signal to noise ratio at least 15. Final cutoff frequency ( $f_c$ ) was determined as  $1/f_c = 1/f_a + 1/f_d$ , where  $f_a$  is analog filter frequency set upon recordings (typically 10 kHz),  $f_d$  - digital frequency (off-line filtering with 8-pole low-pass Bessel filter by pClamp software). Sampling frequency ( $f_s$ ) was reduced to  $f_s = 10 \cdot f_c$ . Recordings with excessive activity, especially fragments with multiple openings, were excluded from analysis. As described in detail in our recent study (Kisiel et al., 2018) GABA-evoked single-channel activity revealed different modes of activity which were also previously reported by Lema and Auerbach (2006). Gating modes clearly differed in open probability and our analysis was limited to the predominant one (showing intermediate open probability, Kisiel et al., 2018). The fact that modal switch could occur during a cluster (or even burst) activity indicates a modulatory process of the same channel rather than activity of distinct receptor subtypes. The latter possibility could be a consequence of expressing receptors with uncanonical stoichiometry (e.g.  $\beta_2\alpha_1\gamma_2\alpha_1\gamma_2$  and  $\beta_2\alpha_1\gamma_2\beta_2\gamma_2$  as reported by Botzolakis et al., 2016) but restriction of our analysis to the dominant mode is expected to eliminate the activity of such receptors from our analysis. Recordings selected for analysis were then idealized by time-course fitting using the SCAN software and information on shut/open intervals was stored in the \*.scn files which were used in subsequent analysis. To construct the open and shut time distributions and to perform fitting of exponential functions, EKDIST program was used. Time resolution for open and shut times was identified separately for each recording and it was in the range of 50-70  $\mu$ s (the dead time for SCAN analysis was 10-30  $\mu$ s shorter, typically in the range 30-60  $\mu$ s) and

these values were then used in the subsequent model simulations. For open time distribution weighted open time constant was calculated with the equation:

$$\tau_{open} = \sum_{i=1}^n P_i \cdot \tau_i \quad \text{Eq. 5}$$

where  $n$  – the number of components,  $P_i$  – area (and respectively percentage:  $P_i\% = 100 \cdot P_i$ ) and  $\tau_i$  – open time of particular ( $i^{\text{th}}$ ) component. Clusters of activity were identified manually (Kisiel et al., 2018). To identify bursts, critical time ( $t_{\text{crit}}$ ) was determined from the shut time distributions of cluster activity which were typically fitted with four components. Jackson’s criterion (Jackson et al., 1983) was most commonly used to determine the critical time (for the 3<sup>th</sup> and 4<sup>th</sup> component in shut time distributions) defining bursts. Microbursts were defined by  $t_{\text{crit}}$  calculated using the same method for the 2<sup>nd</sup> and the 3<sup>rd</sup> component. Individual bursts consisted of several events but they were typically not sufficiently numerous to reliably fit their distributions and for this reason the mean burst duration was calculated as arithmetic average. Open probability was estimated as the ratio of the sum of open time durations and the overall duration of the cluster. The current amplitude corresponding to a particular holding voltage ( $A_{Vhold}$ ) was calculated as a difference in mean amplitudes for open and closed states and the conductance was estimated as the slope of linear regression:  $A_{Vhold} = f(V_{hold})$ .

### 3. 4. Model simulations

Model simulations for macroscopic currents were performed using ChanneLab2 (Synaptosoft) software. The model framework was based on the scheme proposed in our recent study – “flipped” Jones-Westbrook’s model (fJWm; Szczot et al., 2014) with one flipped, one open and one desensitized state connected with a flipped state. The linear model (with a desensitized state originating from an open state) was excluded as it does not explain some macroscopic observations for responses mediated by GABA<sub>A</sub>Rs e.g. experiments with pentobarbital by Feng et al. (2004) and for mutations which uncouple desensitization from deactivation (Bianchi et al., 2007). Since our present study is based on the analysis of responses evoked by saturating agonist concentrations, at which conformational transitions between singly bound states are expected to occur at a low probability, the singly bound states were omitted. A possibility that this assumption could be not fulfilled is discussed for the cysteine mutant (see chapters 4.5 in Results and 5.3 in Discussion). The values of rate constants for recordings made at pH 7.2 were constrained as estimated by (Szczot et al., 2014). To reproduce our results at different pH values, the rate constants were altered to best reproduce the kinetic features of recorded current responses (amplitudes, onset kinetics, macroscopic desensitization and deactivation) in four groups: WT-GABA, WT-P4S, LEU-GABA, CYS-GABA.

For kinetic simulations of single-channel currents, HJCFIT software (DCWinprogs, maximum likelihood method) was used. Since single-channel recordings allow to distinguish and reliably describe more microscopic states than macroscopic recordings, more extensive kinetic scheme than that from (Szczot et al., 2014) had to be used (with two open and two desensitized states - model 1 from Kisiel et al., 2018). Simulations for pH 7.4 were performed as a part of our previous study (Kisiel et al., 2018). Model simulations for pH 6.0 were based on the same kinetic schemes established for pH 7.4 and specified in the mentioned work. Rate constants were fitted to the lists of events (uploaded as \*.scn files) with rate constants evaluated for pH 7.4 by Kisiel et al. (2018, Table 2 in the cited paper) as initial guesses. The assessment of model fitting was based on comparisons between experimental data (open and shut time distributions) and distributions predicted by the model.



### 3. 5. Statistical analysis

SigmaPlot 11.0 (Systat Software) and Excel 2010 (Microsoft) software were used to perform the statistical analysis. Comparisons between groups were performed using the Student t-test. Fisher test was used to compare variances of two groups and to choose the type of t-test (2 or 3). For paired data (from the same patch) Student's t-test type 1 was used. The confidence interval was set at 0.05. The results are expressed as mean  $\pm$  SEM.

### 4. Results

To assess the impact of changes in extracellular pH on WT and mutated receptors, first macroscopic currents were analyzed. As expected, for WT ( $\alpha_1\beta_2\gamma_2$ ) receptors, amplitudes of currents elicited by saturating GABA concentration (10 mM for pH 7.2 and 8.0, 30 mM for pH 6.0) decreased with pH (Fig. 1A1 left), being much larger for acidic pH (pH 6.0, relative amplitudes with respect to those at control pH 7.2:  $2.00 \pm 0.10$ ,  $p = 0.01$ , Fig. 1B) and markedly smaller for basic pH when compared to control conditions (pH 8.0, relative amplitude:  $0.70 \pm 0.13$ ,  $p = 0.02$ , Fig. 1B). These data are thus in agreement with previous reports (Mercik et al., 2006; Mozrzymas et al., 2003b; Pasternack et al., 1996). We have additionally checked effect of protons on currents evoked by a saturating dose of a partial agonist, P4S (1 mM). Modulation of these currents by extracellular pH was qualitatively similar to that observed for GABA-evoked responses, although a trend of a larger increase at acidic and smaller reduction at basic pH values was observed (relative value for pH 6.0:  $2.72 \pm 0.491$ ,  $p = 9 \cdot 10^{-3}$ ; for pH 8.0:  $0.91 \pm 0.13$ ,  $p = 0.03$ , Fig. 1A1 right, B). However, relative changes determined for GABA and P4S at pH 6.0 and 8.0 did not reach statistical significance (respectively  $p = 0.19$  and  $p = 0.26$ ).

Next, we have checked how mutation at the  $\alpha_1$ Phe64 residue affected pH sensitivity of amplitudes for currents elicited by saturating either [GABA] or [P4S]. For leucine mutation ( $\alpha_1$ Phe64Leu), the general trend of amplitude reduction at increasing pH was maintained (Fig. 1A2) but the relative increase at pH 6.0 (for saturating GABA, 100 mM) was much smaller than for WT receptors ( $1.22 \pm 0.07$ , vs. pH 7.2:  $p = 0.04$ , vs. WT:  $p = 2 \cdot 10^{-5}$ , Fig. 1B). For basic pH, relative amplitude reduction of currents mediated by the leucine mutants was similar to that observed for WT receptors ( $0.77 \pm 0.06$ ,  $p = 0.04$  - comparison with pH 7.2, Fig. 1B). Analogous recordings were made for responses mediated by leucine mutants and evoked by saturating concentration of P4S. For this partial agonist, acidic pH markedly enhanced the current amplitude ( $1.77 \pm 0.10$ ,  $p = 0.02$ , Fig. 1B) and this increase was significantly larger than that observed for GABA as agonist ( $p = 4 \cdot 10^{-4}$ ) for this mutant. Basic pH reduced P4S-evoked current amplitude to a similar extent as in the case of GABA ( $0.67 \pm 0.05$ ,  $p = 0.04$ , vs. GABA:  $p = 0.26$ , Fig. 1B). The effect of pH on current amplitude was additionally checked for current responses elicited by high [GABA] (100 mM) and saturating [P4S] (10 mM) for the cysteine mutants ( $\alpha_1$ Phe64Cys, Fig. 1A3, B). Interestingly, at pH 6.0, in contrast to previously considered receptors, no significant increase in current amplitude was observed (relative amplitude for GABA:  $1.18 \pm 0.12$ ,  $p = 0.23$ ; for P4S:  $1.48 \pm 0.14$ ,  $p = 0.14$ ) and highly significant difference was observed between the effect of pH 6.0 in WT and in the cysteine mutants ( $p = 10^{-3}$  for GABA,  $p = 0.04$  for P4S, Fig. 1B). Conversely, the effect of basic pH on GABA- and P4S-evoked currents mediated by the cysteine mutants was markedly stronger than for WT receptors (GABA:  $0.24 \pm 0.04$ , vs. pH 7.2:  $p = 0.01$ ; vs. WT:  $p = 9 \cdot 10^{-3}$ ; P4S:  $0.40 \pm 0.08$ , vs. pH 7.2:  $p = 0.04$ , vs. WT:  $p = 6 \cdot 10^{-3}$ , Fig. 1).

These data show that both for WT and mutated receptors a monotonic decrease of current amplitudes (evoked by saturating concentration of full or partial agonists) with extracellular pH is observed. However, in the case of WT receptors and leucine mutants a

trend toward a larger increase at acidic pH can be observed when the partial agonist is used. Moreover, amplitude modulation by acidic pH is reduced in the leucine mutants and abolished in cysteine ones whereas the sensibility to basic pH was particularly strong in the latter ones.

#### 4. 1. Non-stationary analysis of variance shows that pH reduction increases maximum channel open probability

Current amplitude can be affected by altered single-channel conductance and/or maximum open probability. In our recent study (Szczoł et al., 2014) we have estimated that for  $\alpha_1\beta_1\gamma_2$  receptors in our expression model, the maximum open probability ( $P_{\text{OpenMax}}$ ) was  $\sim 0.65$ . It is thus puzzling to observe a nearly 2-fold increase in amplitude mediated by these currents at pH 6.0 (Fig. 1B) and it may be expected that this change could result from change of both  $P_{\text{OpenMax}}$  and the single-channel conductance. Mortensen et al. (2010) has previously observed an increase in the single-channel conductance for other GABA<sub>A</sub>R types although at a much more acidic pH value (4.0). To check this possibility we performed single-channel recordings from currents evoked in WT receptors by saturating [GABA] at two pH levels (6.0 and 7.4). However, single-channel analysis did not confirm the impact of pH changes on the conductance (pH 7.4:  $24.7 \pm 1.5$ ,  $n = 6$ ; pH 6.0:  $20.6 \pm 3.4$ ,  $n = 11$ , data not shown). To assess the impact of protons on maximum open probability in dynamic conditions, non-stationary analysis of variance for currents mediated by WT receptors and evoked by applications of saturating [GABA] was performed. We observed that acidification significantly increased  $P_{\text{OpenMax}}$  (pH 8.0:  $0.53 \pm 0.03$ ; pH 7.2:  $0.67 \pm 0.04$ , pH 7.2 vs. pH 8.0:  $p = 0.03$ ; pH 6.0:  $0.81 \pm 0.03$ , pH 7.2 vs. pH 6.0:  $p = 0.02$ , data not shown). However, the effect of pH on the open probability indicated by NSVA, is still insufficient to reproduce the observed extent of amplitude increase at pH 6.0 for WT receptors. Thus NSVA provides only a qualitative indication about increased open probability upon acidification but it is insufficient to clarify the underlying mechanisms which we further pursued by combining macroscopic and single-channel analysis (see below).

#### 4. 2. Acidification slows down the onset kinetics of currents mediated by WT receptors and evoked by GABA or P4S

Onset of responses to saturating [GABA] is known to be very fast and therefore recordings aiming at determining the 10-90% Rise Time were performed in the excised patch (outside-out, see Methods) configuration. We found that in the case of WT receptors, acidification slowed down the onset kinetics but alkalization was ineffective (Fig. 2). The effect of acidification is particularly strong when a partial agonist (P4S) was used. 10-90% Rise Time of currents mediated by WT receptors and evoked by GABA application at pH 7.2 was  $0.37 \pm 0.03$  ms; at pH 6.0:  $0.46 \pm 0.04$  ms ( $p = 0.02$ ) and at pH 8.0:  $0.33 \pm 0.04$  ms (pH 7.2 vs. pH 8.0:  $p = 0.58$ ). In the case of WT receptors, acidification caused thus nearly 2-fold slow-down of the onset of currents elicited by P4S – for pH 7.2 10-90% Rise Time was  $1.15 \pm 0.13$  ms and for pH 6.0:  $1.97 \pm 0.18$  ms ( $p = 3 \cdot 10^{-3}$ , vs. GABA:  $p = 0.01$ ) but the effect of alkalization was negligible (pH 8.0:  $1.07 \pm 0.10$  ms, vs. 7.2:  $p = 0.69$ ) similar to that observed for GABA.

#### 4. 3. Acidification reduces the rate and extent of macroscopic desensitization

In agreement with our previous data (Mozrzymas et al., 2003a, 2003b; Szczoł et al., 2014) current responses mediated by the WT receptors and elicited by prolonged applications of saturating [GABA] in control conditions were characterized by a fast onset and a rapid and profound macroscopic desensitization (in the present set of recordings  $\tau_{\text{fastDes}}$ :  $2.22 \pm 0.26$  ms,  $n = 23$ ; ss/peak:  $0.31 \pm 0.03$ ,  $n = 20$ , Fig. 3A1 left). Acidification (to pH 6.0) reduced the rate

and the extent of macroscopic desensitization for responses mediated by WT receptors (relative  $\tau_{\text{fastDes}}$ :  $1.68 \pm 0.11$ ,  $p = 2 \cdot 10^{-3}$ ; relative ss/peak:  $1.58 \pm 0.12$ ,  $p = 3 \cdot 10^{-4}$ , Fig. 3A-C). Alkalization of external medium (to pH 8.0) had a negligible effect on the rapid desensitization time constant (relative  $\tau_{\text{fastDes}}$ :  $0.93 \pm 0.12$ ,  $p = 0.40$ , Fig. 3B) and caused a relatively weak although significant effect on the desensitization extent (relative ss/peak:  $0.85 \pm 0.04$ ,  $p = 0.02$ , Fig. 3C). In our recent study (Szcot et al., 2014) we have found that current responses mediated by WT receptors and evoked by saturating [P4S] were characterized by a slow macroscopic desensitization while the microscopic desensitization (conformational transition) was not abolished and proposed that the manifestation of macroscopic desensitization depended on flipping kinetics. It seems thus interesting to check whether alterations in extracellular pH could affect the desensitization kinetics of currents evoked by P4S. For GABA-evoked currents mediated by WT, the value of FR10 was  $0.34 \pm 0.03$ ,  $n = 22$  (Fig. 3A1 left) whereas for currents elicited by P4S at pH 7.2, typically, were characterized by a weak fading (FR10:  $0.81 \pm 0.04$ ,  $n = 29$ ) with no rapid component (Fig. 3A1 right). Acidification (to pH 6.0) slightly but significantly increased the FR10 value for currents evoked by P4S (relative FR10:  $1.19 \pm 0.08$ ,  $p = 0.01$ ) whereas for GABA-elicited responses this effect was markedly stronger (relative FR10:  $2.07 \pm 0.25$ ,  $p = 3 \cdot 10^{-5}$ , WT-GABA vs. P4S:  $p = 4 \cdot 10^{-3}$ , Fig. 3D). In the case of WT receptors, the effect of alkalization (pH 8.0) was weak for GABA-evoked responses - relative FR10 was  $0.90 \pm 0.04$ ,  $p = 0.045$  and no effect was found for P4S-evoked responses (relative FR10:  $1.02 \pm 0.02$ ,  $p = 0.24$ , WT-GABA vs. P4S:  $p = 8 \cdot 10^{-3}$ , Fig. 3D). Currents mediated by leucine mutants and elicited by GABA application were characterized by a smaller onset rate and extent of desensitization than for WT receptors ( $\tau_{\text{fastDes}}$ :  $6.21 \pm 0.55$  ms,  $n = 18$ , LEU-GABA vs. WT-GABA:  $p = 8 \cdot 10^{-7}$ ; ss/peak:  $0.50 \pm 0.04$ ,  $n = 17$ , vs. WT:  $p = 3 \cdot 10^{-4}$ ; FR10:  $0.64 \pm 0.04$ ,  $n = 18$ , vs. WT:  $p = 4 \cdot 10^{-6}$ , Fig. 3A). Acidic pH increased the FR10 and ss/peak values and prolonged  $\tau_{\text{fastDes}}$  (relative FR10:  $1.32 \pm 0.08$ ,  $p = 3 \cdot 10^{-5}$ , vs. WT:  $p = 0.01$ ; for ss/peak:  $1.33 \pm 0.06$ ,  $p = 10^{-5}$ ; and for  $\tau_{\text{fastDes}}$ :  $2.08 \pm 0.17$ ,  $p = 2 \cdot 10^{-4}$ ; Fig. 3B-D). Notably, for leucine mutants, alkalization (to pH 8.0) produced a clearly stronger effect on desensitization than in the case of WT (relative FR10:  $0.79 \pm 0.03$ ,  $p = 2 \cdot 10^{-4}$ , vs. WT:  $p = 0.04$ ; relative ss/peak:  $0.67 \pm 0.07$ ,  $p = 3 \cdot 10^{-4}$ , vs. WT:  $p = 0.045$ ; relative  $\tau_{\text{fastDes}}$ :  $0.78 \pm 0.05$ ,  $p = 6 \cdot 10^{-3}$ , vs. WT:  $p = 2 \cdot 10^{-3}$ ; Fig. 3B-D). Currents mediated by these mutants and evoked by saturating [P4S] showed no detectable rapid desensitization component (FR10:  $0.96 \pm 0.01$ ,  $n = 13$ ) and alterations of pH within the considered range did not affect the desensitization kinetics (relative FR10 close to unity, Fig. 3D). The same pattern of the lack of rapid macroscopic desensitization (FR10:  $0.98 \pm 0.01$ ,  $n = 43$ ) which was unaffected by extracellular pH was observed also for the cysteine mutant for both GABA and P4S (Figure 3D).

#### 4. 4. Diversified impact of pH changes on deactivation kinetics

Deactivation after a short (1-2 ms) pulse of saturating [GABA] applied to WT receptors is known to show a time course characterized by at least two components, the fast one being in the range of a few milliseconds whereas the slower one is roughly 100 ms (Jones and Westbrook, 1995; Mercik et al., 2006; Mozrzymas et al., 2003b; Szcot et al., 2014). The latter component was implicated as a result of conformational coupling involving opening/closing, desensitization and unbinding (Jones and Westbrook, 1995; Mozrzymas et al., 2007; Scheller and Forman, 2002). In practice, if unbinding is slow enough, sojourns in closed, open and desensitized conformations may take place several times prior agonist unbinding, prolonging deactivation kinetics and reflecting thus a functional “coupling” between these states. Such a complex interdependence between macroscopic current features and rate constants is a consequence of a simple fact that the time course of occupancy of each state is given by a linear combination of exponentials with time constants which potentially

may depend on all elements of the Q matrix (rate constants; Colquhoun and Hawkes, 1995; Colquhoun, 1998). In the present study, deactivation kinetics for responses mediated by WT receptors and evoked by short GABA pulse was characterized by the following biexponential kinetics (Fig. 4A left, for pH 7.2  $\tau_{fast}$ :  $2.79 \pm 0.35$  ms,  $n = 22$ ,  $A_{fast}$ :  $0.70 \pm 0.01$ ,  $n = 25$ ,  $\tau_{slow}$ :  $144 \pm 10$  ms,  $n = 21$ ,  $\tau_{deact}$ :  $45.0 \pm 6.9$  ms,  $n = 19$ ). Acidification from pH 7.2 to 6.0 strongly affected the kinetics of this process (relative  $\tau_{deact}$  was  $2.29 \pm 0.30$  ms,  $p = 10^{-3}$ , Fig. 4B). This change was associated with an increase in the rapid time constant (relative  $\tau_{fast}$ :  $2.71 \pm 0.43$ ,  $p = 0.04$ , Fig. 4C) and a decrease in percentage of the fast component (relative  $A_{fast}$ :  $0.72 \pm 0.06$ ,  $p = 3 \cdot 10^{-3}$ , Fig. 4D) but also a large contribution to prolongation of  $\tau_{deact}$  came from increased percentage of the slow component (relative  $A_{slow}$ :  $1.76 \pm 0.21$ ,  $n = 5$ ,  $p = 0.02$ ) while the value of the slow time constant was only weakly affected (relative  $\tau_{slow}$ :  $1.36 \pm 0.18$ ,  $n = 6$ ,  $p = 0.13$ , data not shown). When alkalinizing the extracellular medium, deactivation kinetics showed a trend to accelerate which was close to the borderline of significance (relative  $\tau_{deact}$ :  $0.72 \pm 0.11$ ,  $p = 0.08$ , Fig. 4B). Deactivation kinetics for currents mediated by WT receptors evoked by short pulses was also determined for the partial agonist P4S. In this case, the pulse duration had to be extended to assure that before agonist removal, the current reaches its maximum value (Fig. 4A right). Deactivation time course at pH 7.2 showed predominantly a biexponential kinetic phenotype ( $\tau_{deact}$ :  $18.1 \pm 0.6$  ms,  $n = 14$ ,  $\tau_{fast}$ :  $5.24 \pm 1.02$  ms,  $n = 14$ ;  $\tau_{slow}$ :  $35.2 \pm 1.4$  ms,  $n = 13$ ,  $A_{fast}$ :  $0.57 \pm 0.03$ ,  $n = 14$ , Fig. 4A right). Consistently with our previous finding (Szczyt et al., 2014) deactivation kinetics after P4S application was much faster than for GABA (relative  $\tau_{deact}$ :  $0.53 \pm 0.08$ ,  $n = 4$ ,  $p = 0.03$ ). This difference resulted primarily from the 4-fold reduction of  $\tau_{slow}$  (relative  $\tau_{slow}$ :  $0.25 \pm 0.04$ ,  $n = 4$ ,  $p = 0.02$ ) compensating a nearly 2-fold increase in the percentage of this component (relative  $A_{slow}$ :  $1.97 \pm 0.04$ ,  $n = 4$ ,  $p = 8 \cdot 10^{-5}$ ), and with more than 2-fold prolongation of  $\tau_{fast}$  (relative  $\tau_{fast}$ :  $2.24 \pm 0.32$ ,  $n = 4$ ,  $p = 0.03$ , data not shown). Acidification to pH 6.0 resulted in a slow-down of deactivation kinetics (relative  $\tau_{deact}$ :  $1.35 \pm 0.08$ ,  $p = 6 \cdot 10^{-3}$ , Fig. 4B) due to significant increase in the fast time constant value (relative  $\tau_{fast}$ :  $1.80 \pm 0.32$ ,  $p = 0.045$ , Fig. 4C) with no impact on a slow component and on the percentage of each component (relative  $\tau_{slow}$ :  $1.20 \pm 0.17$ ,  $n = 9$ ,  $p = 0.29$ ; relative  $A_{fast}$ :  $0.89 \pm 0.16$ ,  $n = 7$ ,  $p = 0.61$ , Fig. 4D). Alkalinization of the extracellular medium had only a relatively weak impact on slow time constant (relative  $\tau_{slow}$ :  $0.85 \pm 0.03$ ,  $n = 10$ ,  $p = 10^{-3}$ ) with no effect on mean deactivation constant (relative  $\tau_{deact}$ :  $0.96 \pm 0.04$ ,  $p = 0.25$ , Fig. 4B). Deactivation of currents evoked by short pulses of saturating agonist and mediated by the leucine mutants showed a single exponential time course both for GABA and P4S (at pH 7.2, for GABA  $\tau_{deact}$ :  $30.6 \pm 2.6$  ms,  $n = 18$ ; for P4S  $\tau_{deact}$ :  $27.3 \pm 2.4$  ms,  $n = 8$ ) and neither acidic nor basic pH affected these time courses (Fig. 4B). In the case of cysteine mutants, GABA- and P4S-evoked current deactivations were monoexponential (at pH 7.2 GABA,  $\tau_{deact}$ :  $12.3 \pm 1.5$  ms,  $n = 25$ ; P4S:  $27.9 \pm 1.83$  ms,  $n = 5$ ). Interestingly, for these mutants, in the case of GABA application, acidic pH had no effect but deactivation kinetics was significantly slowed down when alkalinizing the external solution (relative  $\tau_{deact}$ :  $1.21 \pm 0.07$ ,  $p = 0.03$ , Fig. 4B). Contrary to GABA, deactivation kinetics after short pulses of saturating [P4S] was more sensitive to acidification (pH 6.0 vs. pH 7.2 - relative  $\tau_{deact}$ :  $0.84 \pm 0.02$ ,  $p = 0.04$ , Fig. 4B) than to alkalinization (pH 8.0 vs. pH 7.2 - relative  $\tau_{deact}$ :  $1.04 \pm 0.01$ ,  $p = 0.12$ , Fig. 4B). Thus, for deactivation of currents evoked by short pulses of agonist, mutation at  $\alpha_1$ Phe64 residue leads to enhanced effect of alkaline pH and weaker impact of acidic pH.

In our previous work (Mozrzymas et al., 2007) it has been proposed that the mechanisms of deactivation after short and long applications substantially differ. While in the former case, there is a prominent fast component attributed mainly to rapid desensitization, in the latter one (for applications lasting hundreds of ms) the rapid component is basically lacking and in both cases a slow component, resulting from above mentioned “state coupling”

is present. In our experiments we applied pulses of 500 ms duration and for currents mediated by WT receptors the deactivation kinetics was described by a biexponential function (for GABA -  $\tau_{\text{slow}}$ :  $301 \pm 19$  ms,  $n = 19$ ,  $A_{\text{slow}}$ :  $0.81 \pm 0.04$ ,  $n = 18$ ,  $\tau_{\text{fast}}$ :  $32.4 \pm 6.3$  ms,  $n = 12$ ,  $\tau_{\text{deact}}$ :  $257 \pm 20$  ms,  $n = 19$ ; for P4S -  $\tau_{\text{slow}}$ :  $51.0 \pm 3.8$  ms,  $n = 26$ ;  $\tau_{\text{fast}}$ :  $14.5 \pm 2.3$  ms,  $n = 16$ ;  $A_{\text{slow}}$ :  $0.76 \pm 0.05$ ,  $n = 26$ ;  $\tau_{\text{deact}}$ :  $39.3 \pm 2.4$  ms,  $n = 26$ , data not shown). For mutated receptors, deactivation kinetics after long pulse was monoexponential and with  $\tau$  close to that after short pulse (LEU-GABA -  $\tau_{\text{deact}}$ :  $31.1 \pm 4.0$  ms,  $n = 18$ ; LEU-P4S -  $\tau_{\text{deact}}$ :  $29.9 \pm 3.8$  ms,  $n = 8$ ; CYS-GABA -  $\tau_{\text{deact}}$ :  $13.1 \pm 1.2$  ms,  $n = 42$ ; CYS-P4S -  $\tau_{\text{deact}}$ :  $29.5 \pm 2.7$  ms,  $n = 14$ ; data not shown). Generally, deactivation time course after long agonist pulse showed considerably weaker dependence on extracellular pH than that recorded after short pulses. Indeed, for WT receptors, acidification or alkalization did not influence this process in responses elicited either by GABA or P4S. Interestingly, in the case of leucine mutants alkalization slowed down deactivation kinetics of currents evoked by long GABA pulses (relative  $\tau_{\text{deact}}$  for pH 8.0 vs. pH 7.2:  $1.21 \pm 0.07$ ,  $p = 7 \cdot 10^{-3}$ ) while acidification was ineffective (Fig. 4E). Similar to the leucine mutants, a slow-down of deactivation at basic pH was observed for responses mediated by the cysteine mutants and evoked by GABA (relative  $\tau_{\text{deact}}$ :  $1.29 \pm 0.08$ ,  $p = 9 \cdot 10^{-3}$ , for pH 6.0 no significant effect, Fig. 4E). However, in the case of mutated receptors, deactivation of responses evoked by P4S was not significantly affected either for acidic or alkaline extracellular medium (Fig. 4E). Altogether, deactivation after long pulse showed weaker pH sensitivity than that observed after short agonist application, being resistant to modulation by acidic pH but prolongation of this process by alkaline pH was present in the case of both leucine and cysteine mutants.

#### 4. 5. Simulations based on macroscopic recordings indicate three possible scenarios of GABA<sub>A</sub>R modulation by protons

To interpret our experimental observations, model simulations were made to indicate a minimum requirement model reproducing our results. To this end, we have used the model extensively discussed in our recent study (Szczot et al., 2014).

As we have previously shown (Szczot et al., 2014), flipping/unflipping rate constants ( $\delta_2/\gamma_2$ ) strongly influence several key kinetic features of macroscopic currents including current amplitude, onset kinetics, macroscopic desensitization and deactivation. Notably, all these parameters are affected by protons raising the possibility that GABA<sub>A</sub>R modulation by pH alterations may concern flipping transitions. Indeed, using the scheme (Fig. 5A) and the set of kinetic rate constants estimated by Szczot et al. (2014), even weak changes of  $\delta_2$  cause prominent alterations of all these parameters. In particular, our simulations indicate that a decrease in  $\delta_2$  results in reduction of the current amplitude as well as in diminution of the current onset rate and macroscopic desensitization (Fig. 5B). These predictions, however, do not reproduce our experimental observations as a decrease in current amplitude upon alkalization (Fig. 1) is associated with enhanced desensitization and a trend towards accelerated current onset (Figs. 2, 3). Moreover, a strong upregulation of current amplitude at acidic pH (Fig. 1) is accompanied by a marked down regulation of onset and desensitization rates (Figs. 2, 3). Thus, alterations of the flipping rate  $\delta_2$  yield conflicting predictions regarding current amplitudes and the time course of measured responses, suggesting that protons affect other conformational transitions. However, it needs to be considered that potentially all rate constants in the scheme may shape (to a different extent) any kinetic feature of the macroscopic currents (Colquhoun, 1998; Mozrzymas et al., 2003a). Thus, considering a relatively complex gating scheme (Fig. 5A), the potential impact of each individual rate constant (or group of rate constants) needs to be addressed.

Considering the model 1 (Fig. 5A) with initial parameters from (Szczot et al., 2014), we performed trend simulations aiming at determining how strong is dependence of particular kinetic features of the macroscopic currents on specific rate constants (Fig. 5). In the case of WT receptors current amplitude, macroscopic desensitization, onset and deactivation kinetics were particularly sensitive to changes of  $\delta_2$ ,  $\beta_2$  (channel opening),  $\alpha_2$  (channel closing),  $d_2$  (microscopic desensitization) while changes of  $\gamma_2$  (exit from flipped state) and  $k_{\text{off}}$  (unbinding) strongly affected only deactivation kinetics, and  $r_2$  rate constant (resensitization) – the extent of desensitization (intensity of steady-state current upon prolonged application of saturating agonist) – Fig. 5B-D. Considering these predictions, we made an attempt to ascribe respective changes in the rate constants to observed kinetic effects of protons on the time course of macroscopic currents. In particular, we checked whether rate constants shaping channel opening and closing ( $\beta_2/\alpha_2$ ) and entry into desensitized state ( $d_2$ ) were compatible with the observed effects of protons. Simulations were performed for 4 sets of receptors/agonists – WT-GABA, WT-P4S, LEU-GABA, CYS-GABA (Table 1). Decrease in  $d_2$  in all examined cases caused an increase in current amplitudes, slow down of the onset and macroscopic desensitization kinetics (observations typical for acidification). However, a decrease in  $d_2$  resulted in acceleration of deactivation kinetics, contrary to what observed when lowering pH to 6.0. This discrepancy indicates that alteration in  $d_2$  rate constant alone is not sufficient to reproduce the effect of protons on the macroscopic currents. Previously, it was postulated that pH affects  $d_2/r_2$  and also binding kinetics ( $k_{\text{on}}$  and  $k_{\text{off}}$ , Mozrzymas et al., 2003b). However, simulations presented by Mozrzymas et al. (2003b) were based on the model without the flipping transition. Notably, an important novel feature of the “flipped” model is that the exit from directly activable conformation ( $A_2F$ , Fig. 5A) takes place via unflipping while the receptor remains fully bound, whereas in the previous model (Mozrzymas et al., 2003b) – by unbinding. Thus, the reproduction of deactivation pH-dependence requires considering additionally the unflipping  $\gamma_2$  rate constant. Qualitative reproduction of acidification/alkalization effects for WT receptors on amplitudes and time course of responses could be obtained by decreasing/increasing of both rate constants  $d_2$  and  $\gamma_2$  (Fig. 5C). Table 1 (column “WT – GABA”) shows the values of these rate constants assuring the reproduction of our observations (simulated relative changes of FR10,  $\tau_{\text{deact}}$ , 10-90% Rise Time and  $P_{\text{OpenMax}}$  consistent with experiment). Analogous qualitative data reproduction could be obtained when altering  $d_2$  and  $k_{\text{off}}$  (scenario Ib in the Table 1, not shown in Fig. 5). However, the scenario Ib required large changes in  $k_{\text{off}}$  which, in turn, would give rise to a substantial alteration of agonist affinity beyond our previous estimations (Mozrzymas et al., 2003b). Considering the similarity in predictions by scenario based on alterations of  $d_2/\gamma_2$  and  $d_2/k_{\text{off}}$  they were considered as two variants of the same scenario (Ia and Ib) with a possibility that both  $\gamma_2$  and  $k_{\text{off}}$  are affected. It needs to be added that besides major changes in  $d_2$  and  $\gamma_2/k_{\text{off}}$  rate constants, this scenario required additionally minor modifications of the resensitization rate constant  $r_2$  but no changes in  $\delta_2$  were needed (Table 1, column “WT – GABA”). Importantly, the same mechanisms could be used to qualitatively reproduce the impact of changes in pH on currents elicited by the partial agonist P4S for WT and for responses mediated by LEU mutants and evoked by GABA (Table 1). Interestingly, in the case of CYS mutants, the scenario Ib (in contrast to Ia) did not allow us to reproduce four-fold reduction of current amplitude upon alkalization. The explanation of this difference is that  $\alpha_1\text{Phe64Cys}\beta_2\gamma_2$  receptors are characterized by very slow flipping transitions (in contrast to WT-GABA) which are the major limiting factor for the receptor to get activated and in these conditions open probability strongly depends on both  $d_2$  and  $\gamma_2$  but not on  $k_{\text{off}}$ . It is worth noting that in the case of WT receptors, when saturating [GABA] is applied, acidification from control pH to 6.0 would be accompanied with larger change of both  $d_2$  and  $\gamma_2$  (about 4-fold) than in the case of P4S (about 2.5-fold change) or in the case of mutated receptors (lower than 1.5-fold). The

opposite situation is predicted for alkalization to 8.0 – for most of examined groups (except cysteine mutants)  $d_2$  and  $\gamma_2$  increase less than 2 times. On the other hand, scenario Ib predicts larger changes of  $k_{off}$  in the case of P4S than for GABA at acidification (WT-GABA – 6-fold, WT-P4S – more than 20-fold reduction; at alkalization: WT-GABA – more than 3-fold, WT-P4S – 2.5-fold  $k_{off}$  increase). In the case of  $\alpha_1$ Phe64Leu $\beta_2\gamma_2$  receptors the impact of acidification on  $d_2$ ,  $\gamma_2$  and  $k_{off}$  seems to be weaker than for wild-type receptors (LEU-GABA: less than 2-fold decrease of mentioned rate constants; at alkalization similar changes were observed). Surprisingly, simulations suggest that in the case of  $\alpha_1$ Phe64Cys $\beta_2\gamma_2$  receptors alkalization to pH 8.0 would be connected with more than 6-fold increase in  $d_2$  and almost 4-fold increase of  $\gamma_2$  (Table 1). However, these simulations for the CYS mutant need to be interpreted with caution as they are based on model fitting postulating that at high [GABA] used (100 mM) all receptors reach fully bound states which was recently found to be problematic due to particularly low flipping rate (Kisiel et al., 2018). This issue is discussed in detail in Discussion (chapter 5.3).

Extensive trend analysis performed using model 1 (Fig. 5A) revealed that several major observations concerning modulatory effects of changes in extracellular pH can be reproduced by an alternative scenario - by altering the  $\beta_2$  rate constant (for WT receptors). This scenario has been discarded in our previous paper on proton effects on neuronal GABA<sub>A</sub>Rs (Mozzrymas et al., 2003b) as for the values of rate constants optimized to these data in the classic Jones and Westbrook model, increase in  $\beta_2$  (to reproduce effects of acidification) would lead to the onset acceleration for responses to saturating [GABA], contrary to experimental findings. However, using the flipped model with rate constants adapted to the present data (Fig. 5A), increase in  $\beta_2$  alone predicted a slow-down of the rising phase. Moreover, as shown in Fig. 5D, increase in this rate constant resulted in increased amplitude and a slow-down of deactivation and macroscopic desensitization in agreement with the present findings. Reproduction of our observations concerning the impact of acidification on GABA-evoked responses mediated by the WT receptors would require a robust change in the  $\beta_2$  rate constant but for P4S-elicited responses these changes were smaller and required additionally a decrease in  $\alpha_2$  and a slight increase in  $\gamma_2$  (Table 1). Alkalization to pH = 8.0 could be reproduced by a decrease in  $\beta_2$  for WT receptors and leucine mutants but for cysteine mutants, for which 4-fold decrease in current amplitude was observed (Fig. 1), almost 5-fold decrease in  $\beta_2$  was needed. Again, as mentioned above, this different prediction for the CYS mutant could result from a different pH-sensitivity of non-fully-bound receptors whose activity could be predominant even at high [GABA] (Kisiel et al., 2018). Similar to effect on P4S-evoked currents mediated by WT receptors, in the case of the  $\alpha_1$ Phe64 mutants (activated by GABA) a reproduction of alkalization effects required, besides increase in  $\beta_2$ , a decrease in the  $\alpha_2$  closing rate (Table 1). In addition, in all groups except for WT-GABA a relatively minor correction in the unflipping rate constant  $\gamma_2$  was additionally needed (Table 1). It is worth noting that two proposed mechanisms assume changes of  $\gamma_2$  in opposite directions (at acidification for first scenario – decrease, for second one – increase). However, it seems rather unlikely that whereas the flipping rate  $\delta_2$  is unaffected by changes in pH, the unflipping rate  $\gamma_2$  is.

We also considered the third scenario in which the flipping/unflipping transitions are unaffected by protons but changes in extracellular pH alter primarily  $d_2$  and  $\beta_2$  rate constants (Fig. 5E, Table 1). Interestingly, in this 3<sup>rd</sup> scenario, the major mechanism of modulation of responses mediated by WT receptors was related to alteration of the opening rate  $\beta_2$  but in the case of  $\alpha_1$ Phe64 mutants, a considerably larger sensitivity of desensitization kinetics to pH changes (especially alkalization) was needed (Table 1). It is noteworthy that in this scenario

good qualitative reproduction of our experimental data was achieved by altering only these two rate constants (Table 1).

Taking altogether, macroscopic simulations based on extended model assuming flipping (Szczot et al., 2014) indicate possible mechanisms of pH modulation including most of available gating transitions comprising opening, closing, desensitization and unflipping. However, it remains unclear which out of these three scenarios is really responsible for observed modulation. Taking this into account we decided to extend this study by stationary single-channel recordings and analysis.

#### 4. 6. Protons affect shut time distribution and burst kinetics at saturating [GABA]

Considering above described difficulties in interpreting the model simulations of macroscopic current responses, to get a more clear insight into mechanisms of GABA<sub>A</sub>R modulation by protons, single-channel recordings and analysis were applied. Importantly, the considered scenarios could be applied both to WT and mutants and therefore the single-channel analysis was limited to the WT receptors. In our previous work (Kisiel et al., 2018) we have presented an extensive single-channel analysis of GABA-evoked recordings at control pH. In the present study, in attempt to further explore the mechanisms of proton modulation of receptor gating, we extended these investigations by recordings of single-channel currents elicited by saturating [GABA] (30 mM) at pH 6.0, as macroscopic currents mediated by WT receptors showed a particularly strong sensitivity to acidification. Fig. 6A shows a typical single-channel activity evoked by saturating [GABA] at pH 7.4 and 6.0 for WT receptors. Exemplary open and shut times distributions for events recorded at pH 7.4 and 6.0 are shown in Fig. 6C, D and detailed comparison between respective single-channel characteristics (open and shut time distributions, burst and cluster parameters) is presented in Table 2.

As explained in Theory/calculation, clusters include four shortest components of shut time distributions (typically up to 20-50 ms) and bursts – three components (usually up to 5-10 ms). In the present study we additionally distinguished microbursts which include the fastest closures (typically two components below 1 ms duration). As explained previously (Kisiel et al., 2018), assessment of parameters of the fourth (the longest) shut time component is difficult because of its low percentage and, consequently, in Table 2 we present statistics for the three shorter components. Interestingly, at saturating [GABA], acidification caused a significant burst prolongation and, surprisingly, microburst shortening (Fig. 6A, Table 2). Moreover, open probability clearly increased when lowering pH which is consistent with our results of noise analysis. We also observed an increase in open probability in microbursts (Table 2). As presented in Table 2, there is no significant difference between parameters of experimental open time distributions, including the weighted time constant  $\tau_{\text{open}}$  at the two pH values. However, acidification induced some differences in the shut time distributions at experimental resolution (between 60 and 70  $\mu\text{s}$ ). As it can be seen in Fig. 6A, bursts at pH = 6.0 are characterized by a larger proportion of well-defined closures (visually more closures within burst are reaching the baseline). This effect is due to a larger percentage of the third component of closures although the respective time constant is shortened (Table 2). There was also a trend to shorten the first and the second component of shut times with acidification but it did not reach a statistical significance (Table 2).

##### 4. 6. 1. Analysis of single-channel activity at saturating [GABA] indicates involvement of classical gating but not flipping/unflipping transitions in pH modulation

To interpret described observations in terms of gating mechanism modulation, we performed kinetic model fittings to the experimental data using a model which was introduced



in our recent work (Kisiel et al., 2018) - model 2 with two open and two desensitized doubly bound states (Fig. 6B). First, the rate constants of the model were optimized and then the dwell time distributions were simulated for these models and compared to the experimental distributions (lines superimposed on distributions presented in Fig. 6C, D). Statistics for such simulated probability density functions is disclosed in Table 2 (regular brackets – experimental resolution, square brackets – after correction for missed events, analysis for pH 7.4 from Kisiel et al., 2018). Model fittings showed no differences in open time distributions between recordings performed at pH 7.4 and 6.0 at experimental distributions (and also at resolution 0  $\mu$ s). Our simulations indicate that  $\tau_1$  in the shut times distribution ( $< 100 \mu$ s) is slightly shortened by acidification while  $\tau_2$  ( $\sim 300 \mu$ s) – is not. These observations are consistent with increase of open probability in microbursts (Table 2). Kinetic simulations showed also a lower percentage of closures with the length  $\sim 300 \mu$ s ( $2^{\text{nd}}$  component) at pH 6.0 (only at experimental resolution) and confirmed a higher percentage of third component of closures ( $> 1$  ms, Table 2). However, no effect of pH changes on the time constant of the third shut time component ( $\tau_3$  – a few ms) was revealed although a shortening of this rate constant was observed in experimental distributions. Thus, model 2 allowed us to reproduce our major experimental findings with a minor exception to the shortening of  $\tau_3$  at acidic pH.

As we extensively discussed in our previous work (Kisiel et al., 2018), there is a clear correlation between changes in distribution components with alterations of specific rate constants. Based on these relationships we can make a tentative interpretation of observed pH effects in terms of the rate constants. In particular, change in  $\tau_1$  of the shut time distributions would indicate an alteration in the opening rate constant ( $\beta_2$ ), change in  $P_2$  suggests a modification of unflipping ( $\gamma_2$ ) and change in  $P_3$  could suggest an alteration in the desensitization rate constant ( $d_2$ ). Moreover, the change of  $P_2$ , to some extent, can also result from alteration of the opening  $\beta_2$  or desensitization  $d_2$  transitions what was actually indicated by model fitting (see below). The lack of changes of  $\tau_2$  argues against pH-induced alterations of the flipping rate  $\delta_2$  (Table 3). Our simulations thus indicate that protons accelerate channel opening and desensitization rates without affecting the flipping/unflipping transitions (Table 3). Furthermore, our model simulations confirmed acidification-induced burst prolongation (due to increase in  $\beta_2$ ) and microburst duration reduction (due to increase in  $d_2$ , Table 2). Summarizing, presented results of single-channel recordings reveal the global impact of protons on classical gating but not on flipping/unflipping transitions (Table 3).

Model fitting presented above allowed us to reproduce our major observations at the single-channel level but gave a surprising although consistent prediction regarding the microscopic desensitization. Namely, while for macroscopic currents modeling, scenarios predicting proton effect on this transition, indicated a decrease in  $d_2$  with acidification while at single-channel level the opposite trend is proposed. In our recent study (Kisiel et al., 2018) we have extensively discussed the fact that models optimized for steady-state single-channel data may yield poor predictions for responses elicited by rapid agonist applications, especially with respect to the rate and extent of macroscopic desensitization. Within milliseconds of saturating [GABA] application roughly 70-90% of response undergoes a macroscopic desensitization, the process that is not clearly visible in the steady-state conditions. Notably, the estimates of  $d_2$  rate constant based on fits to the macroscopic non-stationary currents were nearly one order of magnitude larger than those for the steady-state conditions (Tables 1 and 3). Conversely, using the model 1, which adequately reproduced macroscopic recordings, to simulate single-channel data, we would predict an excessively large proportion of closures longer than 1 ms due to high  $d_2$  and slow  $r_2$  rate constants (Fig. 6E, F) which is inconsistent with experimental single-channel distributions (Fig. 6C, D; respective long-duration components highlighted with grey squares). Thus in the steady-state, we could see different

desensitization states (not identified in macroscopic recordings) or just a remnant of desensitization. As we proposed in (Kisiel et al., 2018), it is likely that the number of conformations accessible for GABA<sub>A</sub> receptors are probably markedly larger than in the considered models and imposing extremely different conditions (steady-state vs. responses to ultrafast applications) may result in involvement of non-overlapping sets of conformations and thereby in distinct kinetic behavior predicted by estimated rate constants. This might be particularly relevant with respect to a variety of desensitized states. On the other hand, it is worth emphasizing that the estimation of the rate constants  $\beta_2$ ,  $\delta_2$  and  $\gamma_2$ , which shape two fastest shut time components, based on the single-channel analysis (Kisiel et al., 2018), yielded similar results to those obtained previously using model fitting to macroscopic currents evoked by ultrafast solution exchange (Szcot et al., 2014). This further indicates that the desensitization process in these two extremely different experimental protocols is a major source of discrepancy while estimation of other rate constants is less dependent on experimental conditions.

Summarizing, simulations based on macroscopic and microscopic recordings indicate that the primary mechanism of GABA<sub>A</sub>R gating modulation by protons is the effect on opening and on different forms of desensitization.

## 5. Discussion

### 5. 1. Protons affect gating by modifying desensitization and opening but not flipping

In the present study we have re-addressed the mechanisms of modulation of GABA<sub>A</sub>  $\alpha_1\beta_2\gamma_2$  receptors by changes in extracellular pH by combining macroscopic and single-channel analysis and by considering the novel GABA<sub>A</sub>R kinetic scheme including flipping (preactivation) transition (Kisiel et al., 2018; Szcot et al., 2014). The described here impact of pH changes on the time course of macroscopic GABAergic currents, mediated by neuronal or recombinant  $\alpha_1\beta_2\gamma_2$  receptors, is consistent with that described before (Brodzki et al., 2016; Mercik et al., 2006; Mozrzymas et al., 2003b; Pasternack et al., 1996). The use of a simple Jones and Westbrook's model previously indicated that the major proton effect on the receptor kinetics was to affect the desensitization transition with some impact also on the closing rate and on agonist binding (Mercik et al., 2006; Mozrzymas et al., 2003b). On the other hand, previous reports presenting single-channel data (Huang and Dillon, 1999; Krishek and Smart, 2001) did not indicate any protons impact on closing transitions. It is noteworthy that the resolution of these single-channel recordings was much lower - their shortest shut times were between 1 and 4 ms (while in our analysis two shut components shorter than 1 ms were detected). Thus, it is likely that in these previous analyses the resolution might have been not sufficient to unravel the impact of protons on closed time distributions.

Not surprisingly, an attempt to reproduce the macroscopic observations of pH effect using a more complex model including flipping, gave rise to some difficulties in assigning a unique mechanism, indicating rather a set of scenarios. It points to a common problem in interpreting macroscopic results based on models with a large number of free parameters for which a unique interpretation becomes problematic. We show here that extension of macroscopic investigations with single-channel analysis was a crucial step in solving this problem but a caution should be taken as GABA<sub>A</sub>R kinetic behaviour in dynamic and steady-state conditions shows profound differences, especially with respect to the receptor desensitization. Based on this combined approach, we propose a revision of the mechanism whereby protons affect GABA<sub>A</sub>Rs gating by postulating that, besides the receptor desensitization, opening transition is strongly affected by this factor but no evidence was found for effect on flipping.

The major problem in combining the macroscopic, dynamic data with steady-state single-channel recordings was the issue of desensitization. This problem has been extensively discussed in our recent paper (Kisiel et al., 2018) in which the kinetic model for WT and  $\alpha_1$ Phe64 mutants was constructed based on the single-channel data. In particular, we have shown that desensitization rate constants determined for stationary and dynamic conditions differ by nearly one order of magnitude and, as expected, the model based on steady-state single-channel recordings poorly reproduced the macroscopic desensitization. It needs to be stressed that also other models, based on the single-channel stationary recordings (Dixon et al., 2014, 2015; Keramidas and Harrison, 2010) basically failed to reproduce rapid and profound macroscopic desensitization observed upon rapid application of saturating [GABA] (e.g. Jones and Westbrook, 1995; Mozrzymas et al., 1999; Szczot et al., 2014). In the present study we point to yet additional discrepancy between predictions related to desensitization transitions in the steady-state and dynamic conditions. The simulated shut time distributions for the model based on macroscopic recordings (Szczot et al., 2014), which properly reproduced rapid macroscopic desensitization (with time constant  $\sim 2$ -3 ms), would contain a prominent component of closed events with time constant in the range 20-30 ms (Fig. 6F) which is nearly absent in distributions of single-channel events recorded in the stationary conditions (Fig. 6C). On the other hand, as already mentioned, other gating rate constants such as opening, closing and flipping/unflipping showed only minor differences when estimating them in dynamic (Szczot et al., 2014) or steady-state conditions (Kisiel et al., 2018 and the present study). These observations show that indeed desensitization is the most “neuralgic” aspect when confronting dynamic and stationary GABA<sub>A</sub>R behaviour. It is possible, as we proposed in our previous studies (e.g. Mozrzymas et al., 2003b), that in dynamic conditions, modulation of the desensitization rate could contribute to regulate the current amplitude as a relatively minor increase in open probability observed in the steady-state single-channel activity upon acidification cannot explain a much larger increase in the amplitudes of currents elicited by saturating [GABA] (Fig. 1). However, the present data and modelling, both dynamic and stationary, indicate a novel mechanism in which, besides desensitization, protons would affect primarily the opening rate  $\beta_2$  (Table 3). As already mentioned, our analysis and model simulations indicate that flipping and unflipping transitions are not clearly affected by protons. On the other hand, the kinetic model including the preactivation step, for the rate constants estimated for the present data, predicted that the increase in  $\beta_2$  gave rise to a slow-down of the rise time, in agreement with the experimental data, whereas classic Jones and Westbrook’s model gave an opposite prediction (Mozrzymas et al., 2003b). Thus, even if changes in pH do not clearly affect flipping/unflipping rate constants, the extended kinetic model including these transitions allowed us to obtain a better reproduction of experimental data, indicating a novel scenario postulating a major proton impact on the opening rate. Considering the trends presented in the scenario Ib, it cannot be excluded that protons could modify to some extent the unbinding rate but, as already mentioned, such a robust modification of  $k_{off}$  as presented in Table 1 for this scenario is unlikely because it would predict a strong change in GABA-sensitivity of this receptor.

## 5. 2. Impact of pH on current amplitudes

Impact of changes in extracellular pH on currents elicited by a high [GABA] has been studied in several reports and it is worthwhile to compare them to the present findings. Chen and Huang (2014) reported that lowering pH from 7.3 to 6.4 caused only a weak increase of currents elicited by 1 mM GABA whereas at low [GABA] acidification reduced and alkalization increased current responses. The reason for discrepancy at high [GABA] is not clear although it needs to be emphasized that recordings of Chen and Huang (2014) were made from hypothalamic neurons and they used a relatively slow application system which

practically precluded the detection of rapid current characteristics such as e.g. rapid macroscopic desensitization within millisecond time scale. Notably, however, their observations for currents evoked by low [GABA] (at which application speed was less critical) are in qualitative agreement with our observations made in similar conditions on hippocampal cultured neurons (Mozrzymas et al., 2003b). A similar trend for amplitude upregulation at acidic pH for responses evoked by high [GABA] was reported for acutely dissociated pyramidal neurons (Pasternack et al., 1996). There were some qualitative difference between pH effect in our report (Mercik et al., 2006; Mozrzymas et al., 2003b) and that of Feng and Macdonald (2004) in which no significant amplitude increase was found for currents elicited by 1 mM GABA upon acidification. However, Feng and Macdonald (2004) expressed receptors with different beta subunit ( $\beta_3$ ) which generated responses lacking rapid desensitization component which was predominant in our recordings. It is worth noting that the type of  $\beta$  subunit is crucial for pH modulation (Krishek et al., 1996) and therefore receptors with  $\beta_2$  and  $\beta_3$  can be differently affected by protons although such a comparison has not been systematically studied. Notably, Huang and Dillon (1999) have reported that alkalization (from pH 7.3 to 7.9) caused acceleration of desensitization kinetics of currents mediated by  $\alpha_1\beta_2\gamma_2$  receptors and evoked by 500  $\mu$ M GABA which is consistent with our observations.

Whereas (Mortensen et al., 2010) showed that acidic pH may increase the conductance of GABA<sub>A</sub>Rs, this finding was not confirmed by our single-channel analysis. However, it needs to be pointed out that single-channel recordings presented by Mortensen et al. (2010) were performed under different ionic conditions than in our study (outside-out, here: cell-attached patches). Moreover, Mortensen et al. (2010) showed that acidic pH may increase the conductance of GABA<sub>A</sub>Rs but they made this observation at much lower pH (4.0) and used receptors with different subunits combination ( $\alpha_1\beta_3\gamma_2$ ) which can be differently modulated by protons than  $\alpha_1\beta_2\gamma_2$ . On the other hand, amplitude increase of macroscopic currents for WT receptors at pH 6.0 with respect to control conditions (pH 7.2) was larger than that for  $P_{OpenMax}$  estimated with noise analysis. It is puzzling because single-channel recordings argued against any major pH-dependence of the channel conductance. This implies that estimations made using the analysis of variance should be interpreted as a qualitative rather than strictly quantitative estimation, at least in our experimental conditions.

Yet another surprising result was that the values of single-channel conductance estimated here were relatively low (24.7 pS). However, other authors indicated similar values on the basis of single-channel recordings: ~24 pS (Lema and Auerbach, 2006), ~26 pS (Dixon et al., 2014), ~27 pS (Mortensen et al., 2004). Interestingly, relatively low conductance (~24 pS) was determined by (Lema and Auerbach, 2006) in the cell-attached configuration (like in our case), whereas higher ones: ~26 and ~27 pS (Dixon et al., 2014; Mortensen et al., 2004) were measured from excised patches. It cannot be thus excluded that cell-attached configuration might influence the measured current amplitudes. In this mode, such parameters as the membrane potential, the intracellular chloride and bicarbonate concentrations (and thereby the reversal potential for GABA-induced currents) are unknown and cannot be controlled. In addition, it cannot be excluded that ion conduction through the patch might affect the resting potential – such a scenario has been reported for cells characterized by a high input resistance (Fenwick et al., 1982; Mozrzymas et al., 1997). Moreover, at highly positive pipette potentials applied here, the membrane patch is expected to be strongly hyperpolarized and the predominant component of chloride ions would flow outwardly (inward current). Since intracellular concentration of chloride ions is expected to be considerably lower than the extracellular one, the current amplitude measured at strongly negative membrane potentials may be lower than for outward currents (a rectification

predicted by Goldman-Hodgkin-Katz current equation, see e.g. in Hille, 2001) therefore giving rise to conductance underestimation.

In the case of P4S-elicited currents mediated by leucine mutants, acidification caused a larger relative increase in amplitude than in the case of GABA (Figure 1). A similar trend was observed for WT receptors. Our model simulations provide a plausible interpretation of this finding. In the case of P4S, for which the occupancy of the flipped state is low (because of low  $\delta$ ), acidification causes a large relative increase in the flipped state occupancy, whereas in the case of GABA, for which  $\delta$  and flipped state occupancy are higher at physiological pH, the relative increase due to acidification is smaller (simulations not shown).

### 5. 3. Mutations of $\alpha_1$ Phe64 alter receptor sensitivity to alkalization

Interestingly, mutations of  $\alpha_1$ Phe64 residue appear to make various aspects of the receptor functioning (manifested macroscopically as amplitude, desensitization and deactivation) more sensitive to alkaline pH which is particularly evident for the cysteine mutant (Figs. 1, 3, 4). It is noteworthy that cysteine –SH group can dissociate with  $pK_a = 8.37$  implying that at pH 8.0 a part of receptors would be negatively charged. This could explain stronger impact of alkaline pH on cysteine mutants in comparison with WT and leucine mutants. However, a prolongation of deactivation time constant ( $\tau_{deact}$ ) after long pulse was also observed for the leucine mutant (Fig. 4E), indicating that ionization of the sulphhydryl group at the cysteine residue could not be a sole mechanism underlying increased sensitivity to alkalization. Especially analysis of deactivation kinetics reveals how subtle and complex the mechanism of modulation by changes in extracellular pH is. The mechanism emerging from these studies points to alterations of  $d_2$  and  $\beta_2$  rate constants. However, changes in these parameters can cause acceleration, slow-down or no changes in deactivation kinetics, as a modification of each of them separately may produce opposite effects on this process and the overall result depends on the balance between their impacts. It is worth emphasizing that mutations of  $\alpha_1$ Phe64 residue seem to enhance the sensitivity especially of  $d_2$  rate constant to alkaline pH. This is surprising as it has been recently proposed by Gielen et al. (2015) that the desensitization gate is very distant from the binding site and is regulated by interactions between the second and third transmembrane segments affecting the channel lumen close to its intracellular side. Thus, mutation of  $\alpha_1$ Phe64 residue have far reaching, distant from the binding site structural consequences, affecting thereby late stages of receptor gating including opening and desensitization. On the other hand, it is worth noting that simulations based on macroscopic recordings were carried out under the assumption of saturating conditions while in our recent paper (Kisiel et al., 2018) we postulated that at 100 mM of GABA (used in macroscopic recordings for mutated receptors), in the case of  $\alpha_1$ Phe64Cys $\beta_2\gamma_2$ , activity of singly bound GABA<sub>A</sub>R is particularly abundant. Thus, for this mutant, altered pH-sensitivity could reflect, at least in part, the properties of singly bound receptors. This could be an additional aspect of different sensitivity of  $d_2$  and  $\beta_2$  rate constants to pH in the case of WT receptors and cysteine mutants.

It needs to be pointed out that considered here  $\alpha_1$ Phe64 residue is not the only one implicated in GABA<sub>A</sub>R pH-sensitivity. The structural determinants of pH modulation are present at GABA binding site:  $\beta_2$ Tyr205,  $\alpha_1$ Phe66 and  $\alpha_1$ Phe64 (Huang et al., 2004) but there are also some charged residues in the vicinity of the channel gate:  $\beta_2$ His267,  $\beta_2$ Lys279 (Wilkins et al., 2005). It cannot be excluded that a concomitant interaction of protons with these residues may exert a global effect on GABA<sub>A</sub>R macromolecule comprising large portions of the channel structure and thereby to affect its gating. This hypothesis is somehow reminiscent of proposal by Xiu et al. (2005) that at the interface of Cys-loop receptors the

overall charging pattern is crucial to transmit the conformational transition rather than any specific, singular electrostatic interactions.

## 6. Conclusions

The present study combines high resolution, dynamic macroscopic recordings and single-channel investigations to extend our knowledge on mechanisms whereby protons affect GABA<sub>A</sub>R gating. We show that, in addition to binding transitions and desensitization (Mozrzymas et al., 2003b), protons markedly affect also receptor opening, altering thus its efficacy.  $\alpha_1$ Phe64 residue is involved in pH-sensitivity of this receptor gating implying that mutation at this binding site residue strongly affect distant parts of the channel macromolecule which are believed to be involved in late gating transitions of GABA<sub>A</sub>R. Taken altogether, these findings suggest that different conformational transitions and their structural determinants may be strongly coupled and therefore future studies of gating mechanisms will most likely require a more “holistic” approach both at functional and structural level.

## Acknowledgements

*This work was supported by Polish National Science Centre Grants DEC-2013/11/B/NZ3/00983 and UMO-2015/18/A/NZ1/00395 (Maestro) to J.W.M. M.K. was partially supported by Wrocław Medical University Grant Pbm135. J.W.M. was supported by a Foundation for Polish Science mobility grant (3/2015/WSN2014) to visit the laboratory of Prof. Lucia Sivilotti at the University College London. J.W.M was partially supported by statutory funds of Wrocław Medical University (ST.A052.16.023). The authors thank L. Sivilotti for possibility to perform a part of some experiments in her laboratory at the Department of Neuroscience, Physiology and Pharmacology in UCL and R. Lape for his valuable help in introducing DCProgs and DCWinprogs software to our group, and M. Michałowski for technical help in graphics of this paper.*

## References

- Bianchi, M.T., Botzolakis, E.J., Haas, K.F., Fisher, J.L., Macdonald, R.L., 2007. Microscopic kinetic determinants of macroscopic currents: insights from coupling and uncoupling of GABAA receptor desensitization and deactivation. *J. Physiol.* 584, 769–87. doi:10.1113/jphysiol.2007.142364
- Botzolakis, E.J., Gurba, K.N., Lagrange, X.A.H., Feng, H., Stanic, X.A.K., Hu, N., Macdonald, X.R.L., 2016. Comparison of gamma-aminobutyric acid, type A (GABAA), receptor  $\alpha$  $\beta$  $\gamma$  and  $\alpha$  $\beta$  $\delta$  expression using flow cytometry and electrophysiology. *J. Biol. Chem.* 291, 20440–61. doi:10.1074/jbc.M115.698860
- Brickley, S.G., Mody, I., 2012. Extrasynaptic GABAA receptors : their function in the CNS and implications for disease. *Neuron* 73, 23–34. doi:10.1016/j.neuron.2011.12.012
- Brodzki, M., Rutkowski, R., Jatzak, M., Kisiel, M., Czyzewska, M.M., Mozrzymas, J.W., 2016. Comparison of kinetic and pharmacological profiles of recombinant  $\alpha 1\gamma 2L$  and  $\alpha 1\beta 2\gamma 2L$  GABAA receptors – A clue to the role of intersubunit interactions. *Eur. J. Pharmacol.* 784, 81–89. doi:10.1016/j.ejphar.2016.05.015
- Burzomato, V., Beato, M., Groot-Kormelink, P.J., Colquhoun, D., Sivilotti, L.G., 2004. Single-channel behavior of heteromeric  $\alpha 1\beta$  glycine receptors: an attempt to detect a conformational change before the channel opens. *J. Neurosci.* 24, 10924–10940. doi:10.1523/JNEUROSCI.3424-04.2004

- Chen, C., Okayama, H., 1987. High-efficiency transformation of mammalian cells by plasmid DNA. *Mol. Cell. Biol.* 7, 2745–52. doi:10.1128/MCB.7.8.2745
- Chen, J.C.T., Chesler, M., 1992. Modulation of extracellular pH by glutamate and GABA in rat hippocampal slices. *J. Neurophysiol.* 67, 29–36.
- Chen, J.C.T., Chesler, M., 1991. Extracellular alkalinization evoked by GABA and its relationship to activity-dependent pH shifts in turtle cerebellum. *J. Physiol.* 442, 431–446.
- Chen, Z.-L., Huang, R.-Q., 2014. Extracellular pH modulates GABAergic neurotransmission in rat hypothalamus. *Neuroscience* 271, 64–76. doi:10.1016/j.neuroscience.2014.04.028
- Colquhoun, D., 1998. Binding, gating, affinity and efficacy: the interpretation of structure-activity relationships for agonists and of the effects of mutating receptors. *Br. J. Pharmacol.* 125, 924–947. doi:10.1038/sj.bjp.0702164
- Colquhoun, D., Hawkes, A.G., 1995. A Q matrix cookbook: How to write only one program to calculate the single-channel and macroscopic predictions for any kinetic mechanism, in: *Single-Channel Recording*. Springer, pp. 589–633.
- Colquhoun, D., Lape, R., 2012. Allosteric coupling in ligand-gated ion channels. *J. Gen. Physiol.* 140, 625–34. doi:10.1085/jgp.201210849
- Corradi, J., Bouzat, X.C., 2014. Unraveling mechanisms underlying partial agonism in 5HT<sub>3A</sub> receptors. *J. Neurosci.* 34, 16865–76. doi:10.1523/JNEUROSCI.1970-14.2014
- De Koninck, Y., Mody, I., 1994. Noise analysis of miniature IPSCs in adult rat brain slices: properties and modulation of synaptic GABA<sub>A</sub> receptor channels. *J. Neurophysiol.* 71, 1318–35. doi:10.1152/jn.1994.71.4.1318
- DeVries, S.H., 2001. Exocytosed protons feedback to suppress the Ca<sup>2+</sup> current in mammalian cone photoreceptors. *Neuron* 32, 1107–1117. doi:10.1016/S0896-6273(01)00535-9
- Dietrich, C.J., Morad, M., 2010. Synaptic acidification enhances GABA<sub>A</sub> signaling. *J. Neurosci.* 30, 16044–16052. doi:10.1523/JNEUROSCI.6364-09.2010
- Dixon, C., Sah, P., Lynch, J.W., Keramidas, A., 2014. GABA<sub>A</sub> receptor  $\alpha$ - and  $\gamma$ - subunits shape synaptic currents via different mechanisms. *J. Biol. Chem.* 289, 0–23. doi:10.1074/jbc.M113.514695
- Dixon, C.L., Harrison, N.L., Lynch, J.W., Keramidas, A., 2015. Zolpidem and eszopiclone prime  $\alpha 1\beta 2\gamma 2$  GABA<sub>A</sub> receptors for longer duration of activity. *Br. J. Pharmacol.* 172, 3522–3536. doi:10.1111/bph.13142
- Farrant, M., Nusser, Z., 2005. Variations on an inhibitory theme: phasic and tonic activation of GABA(A) receptors. *Nat. Rev. Neurosci.* 6, 215–229. doi:10.1038/nrn1625
- Feng, H., Bianchi, M., Macdonald, R., 2004. Pentobarbital differentially modulates  $\alpha 1\beta 3\delta$  and  $\alpha 1\beta 3\gamma 2L$  GABA<sub>A</sub> receptor currents. *Mol. Pharmacol.* 66, 988–1003. doi:10.1124/mol.104.002543.1980
- Feng, H., Macdonald, R.L., 2004. Proton modulation of  $\alpha 1\beta 3\delta$  GABA<sub>A</sub> receptor channel gating and desensitization. *J. Neurophysiol.* 92, 1577–85. doi:10.1152/jn.00285.2004
- Fenwick, E.M., Marty, A., Neher, E., 1982. A patch-clamp study of bovine chromaffin cells and of their sensitivity to acetylcholine. *J. Physiol.* 577–597.

- Ghavanini, A., Isbasescu, I., Mathers, D., Puil, E., 2006. Optimizing fluctuation analysis of GABAergic IPSCs for accurate unitary currents. *J. Neurosci. Methods* 158, 150–6. doi:10.1016/j.jneumeth.2006.05.015
- Gielen, M., Thomas, P., Smart, T.G., 2015. The desensitization gate of inhibitory Cys-loop receptors. *Nat. Commun.* 6, 6829. doi:10.1038/ncomms7829
- Gielen, M.C., Lumb, M.J., Smart, T.G., 2012. Benzodiazepines modulate GABA receptors by regulating the preactivation step after GABA binding. *J. Neurosci.* 32, 5707–15. doi:10.1523/JNEUROSCI.5663-11.2012
- Hille, B., 2001. *Ion Channels of Excitable Membranes*, 3rd ed. Sinauer Associates, Inc., Sunderland.
- Hoffman, W.E., Charbel, F.T., Edelman, G., Hannigan, K., Ausman, J.I., 1996. Brain tissue oxygen pressure, carbon dioxide pressure and pH during ischemia. *Neurol. Res.* 18, 54–6.
- Hoffman, W.E., Charbel, F.T., Gonzalez-Portillo, G., Ausman, J.I., 1999. Measurement of ischemia by changes in tissue oxygen, carbon dioxide, and pH. *Surg. Neurol.* 51, 654–658. doi:10.1016/S0090-3019(99)00011-7
- Huang, R.-Q., Chen, Z., Dillon, G.H., 2004. Molecular basis for modulation of recombinant alpha1beta2gamma2 GABA receptors by protons. *J. Neurophysiol.* 92, 883–894. doi:10.1152/jn.01040.2003
- Huang, R.-Q., Dillon, G.H., 1999. Effect of extracellular pH on GABA-activated current in rat recombinant receptors and thin hypothalamic slices. *J. Neurophysiol.* 82, 1233–1243.
- Jackson, M.B., Wong, B.S., Morris, C.E., Lecar, H., Christian, C.N., 1983. Successive openings of the same acetylcholine receptor channel are correlated in open time. *Biophys. J.* 42, 109–14.
- Jadey, S., Auerbach, A., 2012. An integrated catch-and-hold mechanism activates nicotinic acetylcholine receptors. *J. Gen. Physiol.* 140, 17–28. doi:10.1085/jgp.201210801
- Jonas, P., 1995. Fast application of agonists to isolated membrane patches, in: Sakmann, B., Neher, E. (Eds.), *Single-Channel Recording*. Plenum Press, New York and London, pp. 231–243.
- Jones, M. V., Westbrook, G.L., 1995. Desensitized states prolong GABA channel responses to brief agonist pulses. *Neuron* 15, 181–191.
- Kaila, K., 1994. Ionic basis of GABA receptor channel function in the nervous system. *Prog. Neurobiol.* 42, 489–537. doi:10.1016/0301-0082(94)90049-3
- Kaila, K., Voipio, J., 1987. Postsynaptic fall in intracellular pH induced by GABA-activated bicarbonate conductance. *Nature* 330, 163–165. doi:10.1038/330163a0
- Keramidas, A., Harrison, N.L., 2010. The activation mechanism of alpha1beta2gamma2S and alpha3beta3gamma2S GABA receptors. *J. Gen. Physiol.* 135, 59–75. doi:10.1085/jgp.200910317
- Kisiel, M., Jatczak, M., Brodzki, M., Mozrzymas, J.W., 2018. Spontaneous activity, singly bound states and the impact of alpha1Phe64 mutation on GABAAR gating in the novel kinetic model based on the single-channel recordings. *Neuropharmacology* 131, 453–474. doi:10.1016/j.neuropharm.2017.11.030
- Kraig, R.P., Petito, C.K., Plum, F., Pulsinelli, W.A., 1987. Hydrogen ions kill brain at



- concentrations reached in ischemia. *J. Cereb. Blood Flow Metab.* 7, 379–386.  
doi:10.1016/j.biotechadv.2011.08.021.Secreted
- Krishek, B.J., Amato, A., Connolly, C.N., Moss, S.J., Smart, T.G., 1996. Proton sensitivity of the GABAA receptor is associated with the receptor subunit composition. *J. Physiol.* 492, 431–443.
- Krishek, B.J., Smart, T.G., 2001. Proton sensitivity of rat cerebellar granule cell GABAA receptors: dependence on neuronal development. *J. Physiol.* 530, 219–233.
- Lape, R., Colquhoun, D., Sivilotti, L.G., 2008. On the nature of partial agonism in the nicotinic receptor superfamily. *Nature* 454, 722–727. doi:10.1038/nature07139
- Lema, G.M.C., Auerbach, A., 2006. Modes and models of GABAA receptor gating. *J. Physiol.* 572, 183–200. doi:10.1113/jphysiol.2005.099093
- Mercik, K., Pytel, M., Cherubini, E., Mozrzymas, J.W., 2006. Effect of extracellular pH on recombinant  $\alpha 1\beta 2\gamma 2$  and  $\alpha 1\beta 2$  GABAA receptors. *Neuropharmacology* 51, 305–314. doi:10.1016/j.neuropharm.2006.03.023
- Miesenböck, G., De Angelis, D.A., Rothman, J.E., 1998. Visualizing secretion and synaptic transmission with pH-sensitive green fluorescent proteins. *Nature* 394, 192–195.  
doi:10.1038/28190
- Mortensen, M., Ebert, B., Wafford, K., Smart, T.G., 2010. Distinct activities of GABA agonists at synaptic- and extrasynaptic-type GABAA receptors. *J. Physiol.* 588, 1251–1268. doi:10.1113/jphysiol.2009.182444
- Mortensen, M., Kristiansen, U., Ebert, B., Frølund, B., Krosgaard-Larsen, P., Smart, T.G., 2004. Activation of single heteromeric GABA(A) receptor ion channels by full and partial agonists. *J. Physiol.* 557, 389–413. doi:10.1113/jphysiol.2003.054734
- Mozrzymas, J.W., Barberis, A., Mercik, K., Zarnowska, E.D., 2003a. Binding sites, singly bound states, and conformation coupling shape GABA-evoked currents. *J. Neurophysiol.* 89, 871–883. doi:10.1152/jn.00951.2002
- Mozrzymas, J.W., Barberis, A., Michalak, K., Cherubini, E., 1999. Chlorpromazine inhibits miniature GABAergic currents by reducing the binding and by increasing the unbinding rate of GABAA receptors. *J. Neurosci. Off. J. Soc. Neurosci.* 19, 2474–2488.
- Mozrzymas, J.W., Martina, M., Ruzzier, F., 1997. A large-conductance voltage-dependent potassium channel in cultured pig articular chondrocytes. *Pflugers Arch.* 433, 413–27.  
doi:10.1007/s004240050295
- Mozrzymas, J.W., Wójtowicz, T., Piast, M., Lebida, K., Wyrembek, P., Mercik, K., 2007. GABA transient sets the susceptibility of mIPSCs to modulation by benzodiazepine receptor agonists in rat hippocampal neurons. *J. Physiol.* 585, 29–46.  
doi:10.1113/jphysiol.2007.143602
- Mozrzymas, J.W., Zarnowska, E.D., Pytel, M., Mercik, K., 2003b. Modulation of GABA(A) receptors by hydrogen ions reveals synaptic GABA transient and a crucial role of the desensitization process. *J. Neurosci.* 23, 7981–7992.
- Mukhtasimova, N., Lee, W.Y., Wang, H.-L., Sine, S.M., 2009. Detection and Trapping of Intermediate States Priming Nicotinic Receptor Channel Opening. *Nature* 459, 451–454.  
doi:10.1038/nature07923.Detection
- Palmer, M.J., Hull, C., Vigh, J., 2003. Synaptic cleft acidification and modulation of short-term depression by exocytosed protons in retinal bipolar cells. *J. Neurosci.* 23, 11332–

11341.

- Pasternack, M., Smirnov, S., Kaila, K., 1996. Proton modulation of functionally distinct GABAA receptors in acutely isolated pyramidal neurons of rat hippocampus. *Neuropharmacology* 35, 1279–88.
- Robello, M., Baldelli, P., Cupello, A., 1994. Modulation by extracellular pH of the activity of GABAA receptors on rat cerebellum granule cells. *Neuroscience* 61, 833–837.
- Scheller, M., Forman, S.A., 2002. Coupled and uncoupled gating and desensitization effects by pore domain mutations in GABA(A) receptors. *J. Neurosci.* 22, 8411–8421.
- Sieghart, W., 2006. Structure, pharmacology and function of GABAA receptor subtypes. *Adv. Pharmacol.* 54, 231–63.
- Szczot, M., Kisiel, M., Czyzewska, M.M., Mozrzymas, J.W., 2014.  $\alpha$ 1F64 residue at GABAA receptor binding site is involved in gating by influencing the receptor flipping transitions. *J. Neurosci.* 34, 3193–209. doi:10.1523/JNEUROSCI.2533-13.2014
- Wagner, D.A., Czajkowski, C., Jones, M. V., 2004. An arginine involved in GABA binding and unbinding but not gating of the GABA(A) receptor. *J. Neurosci.* 24, 2733–2741. doi:10.1523/JNEUROSCI.4316-03.2004
- Wilkins, M.E., Hosie, A.M., Smart, T.G., 2005. Proton modulation of recombinant GABA(A) receptors: influence of GABA concentration and the beta subunit TM2-TM3 domain. *J. Physiol.* 567, 365–377. doi:10.1113/jphysiol.2005.088823
- Wójtowicz, T., Wyrembek, P., Lebida, K., Piast, M., Mozrzymas, J.W., 2008. Flurazepam effect on GABAergic currents depends on extracellular pH. *Br. J. Pharmacol.* 154, 234–245. doi:10.1038/bjp.2008.90
- Xiu, X., Hanek, A.P., Wang, J., Lester, H.A., Dougherty, D.A., 2005. A unified view of the role of electrostatic interactions in modulating the gating of Cys loop receptors. *J. Biol. Chem.* 280, 41655–41666. doi:10.1074/jbc.M508635200

## Figure legends

**Figure 1.** Acidification increases and alkalization decreases the amplitude of current responses evoked by saturating concentration of full (GABA) or partial (P4S) agonist. A1, typical traces of current responses mediated by wild-type (WT) GABA<sub>A</sub> receptors in response to saturating concentrations of the full agonist – 10 mM (pH 7.2 and 8.0) and 30 mM (pH 6.0) GABA (left) or a partial agonist – 1 mM P4S (right) at different pH values indicated by the gray scale and the inset. A2 and A3, typical currents evoked by 100 mM GABA applied to  $\alpha_1$ F64L (LEU) and  $\alpha_1$ F64C (CYS) mutants, respectively at different pH values. B, statistics for relative amplitude values measured for WT and for mutated receptors at different pH values. Each data point at a given pH value (6.0 or 8.0) represents the relative amplitude which was determined by normalization to the amplitude measured at pH 7.2 from the same cell. Note that for WT, acidic pH tends to exert a larger effect, whereas in mutants, a trend toward a higher sensitivity to alkaline pH is observed. Insets above current traces indicate agonist applications. Asterisks mean a statistically significant difference.

**Figure 2.** The onset kinetics (10-90% Rise Time) of current responses mediated by WT receptors and elicited by saturating [GABA] or [P4S] is slowed down by acidification of extracellular medium whereas alkalization is ineffective. A, typical normalized traces showing a reduction of the onset rate at acidic pH in comparison to control pH for responses evoked by GABA (left) and P4S (right). B, statistics of 10-90% Rise Times for GABA- and P4S-evoked currents. Insets above current traces indicate agonist applications. Asterisks indicate a statistically significant difference.

**Figure 3.** The rate and the extent of rapid desensitization are sensitive to alterations of extracellular pH. A1, A2, typical normalized traces of currents mediated by WT (A1) and LEU (A2) receptors showing fast component of desensitization at pH 6.0, 7.2 and 8.0. When currents are evoked by saturating P4S, the rapid desensitization component is not present for WT receptors. B, statistics of relative fast component of desensitization for acidic and alkaline pH in GABA-evoked currents. Note that for WT receptors the effect of alkalization was not significant and for both receptors, the impact of acidic pH on desensitization is large and significant. C, statistics for saturating [GABA] applications showing that significant differences for both acidic and basic pH are found for relative ss/peak parameter demonstrating the impact of protons on the extent of desensitization. D, statistics for macroscopic desensitization assessed as FR10 parameter. Note that acidification slowed down desensitization kinetics and alkalization accelerated it except for groups showing weak desensitization kinetics (LEU-P4S, CYS-GABA, CYS-P4S). Insets above current traces indicate agonist applications. Asterisks indicate a statistically significant difference.

**Figure 4.** The impact of changes in extracellular pH on the time course of deactivation. A, typical normalized current traces showing deactivation kinetics after a short pulse of saturating [GABA] or [P4S] for WT receptors. Insets above traces indicate agonist applications. Note that in the case of P4S in A, agonist pulse duration was extended to assure that current reaches its maximum value. B, statistics of relative weighted deactivation time constants  $\tau_{deact}$ . Note that in the case of WT receptors, only acidic pH significantly prolonged this parameter whereas in the case of the CYS mutants, alkalization slowed down the deactivation process (when GABA was applied) and acidification to pH 6.0 accelerated it (for P4S application). C, D, statistics for the time constant (C) and its percentage (D) for the rapid component of deactivation following a brief agonist application for WT receptors (deactivation was fitted with a sum of two exponential functions, see Results). E, statistics of relative  $\tau_{deact}$  for current responses elicited by long (500 ms) applications of agonists. Note that similar to B, in the case of GABA-evoked responses for mutants, alkalization slowed down deactivation time course. Asterisks indicate a statistically significant difference.

**Figure 5.** Model simulations for macroscopic currents based on the frame of flipped Jones-Westbrook's model (Szcot et al., 2014). A, the scheme presenting fJW model (model 1) where R – the unbound receptor, A – an agonist, states: F – flipped, D – desensitized, O – open. Drawings B-E show results of model simulations in which controls were simulated as in Szcot et al., (2014). For non-mutated  $\alpha_1\beta_2\gamma_2$  GABA<sub>A</sub>Rs (in E additionally simulations for the CYS mutant is shown) three scenarios described in chapter 4.5 were considered to reproduce the impact of protons on recorded currents. B, simulations of the impact of  $\delta_2$  rate constant decrease (displayed using grayscale) on macroscopic currents evoked by saturating [GABA]. Traces in panels C-D show simulations for two scenarios of pH modulation – in the first  $d_2$  and  $\gamma_2$  are changed either separately (for pH 7.2 in dark grey, C1) or both of them are modified with an additional correction of  $r_2$  (C2), in the second one  $\beta_2$  is altered (D). In chapter 4.5 we additionally described a scenario Ib (not shown in this figure) in which variation of  $d_2/r_2$  and  $k_{off}$  (instead of  $\gamma_2$ ) were considered to make similar predictions. E, simulations for wild-type receptor (upper row) and cysteine

$\alpha_1$ Phe64 mutants (lower row) for the scenario in which protons affect both the open  $\beta_2$  and desensitization  $d_2$  rates. Note a difference in the impact of alkaline pH for WT and the CYS mutants. The rate constants (in  $\text{ms}^{-1}$ , numbers located next to simulated traces) optimized for these scenarios are presented in Table 1. In C, D and E, drawings are made for the rate constants optimized to reproduce currents' features at acidic (black), control (dark grey) and alkaline (light grey) pH values (insets in the gray scale).

Figure 6. The impact of extracellular pH on the single-channel cluster activity at saturating [GABA] for wild-type  $\alpha_1\beta_2\gamma_2$  receptors. A, typical traces of single-channel recordings evoked by saturating [GABA] at pH 7.4 (10 mM) and 6.0 (30 mM). B, modified flipped Jones-Westbrook's model with two doubly bound desensitized and two open states (model 2). R – unbound receptor, A – agonist, states: F – flipped, D, D' – desensitized, O, O' – open. C, D, typical fittings of experimental open and shut time distributions of cluster activity elicited by saturating [GABA] at pH 7.4 (C) and 6.0 (D) performed with model 2. Thin lines present specific components of shut and open time distributions with respective parameters (percentages  $P\% \geq 1$  and time constants  $\tau$ ) at experimental resolution. Grey dashed lines show idealized (at resolution 0  $\mu\text{s}$ ) probability density functions. Data for pH 7.4 are from (Kisiel et al., 2018). E. Gating part of flipped Jones-Westbrook's model (model 1, Szczot et al., 2014, to model  $\text{GABA}_A\text{R}$  at saturating [agonist]) and shut time distribution (F) simulated for this model at resolution 60  $\mu\text{s}$ , using the rate constants evaluated from macroscopic recordings by Szczot et al. (2014). Note that for saturating [GABA], the model based on macroscopic recordings (E) predicts a very prominent shut time component ( $\tau_3$ , F) which is very small in distributions of shut times determined in the single-channel recordings (C and D, grey boxes). This difference points to distinct involvement of desensitization transitions in dynamic conditions (rapid agonist applications) and single-channel recordings in stationary conditions (see chapters 4.5, 4.6 and 5.1).

## Tables

**Table 1. Rate constants of flipped Jones-Westbrook's model reproducing macroscopic currents mediated by WT, LEU and CYS receptors and evoked by saturating concentrations of GABA or P4S for various pH values. Rate constants for pH 7.2 were evaluated by (Szczot et al., 2014). Since fitting was performed for saturating concentrations of agonists, the binding rate constants were not relevant and were not disclosed in the table. The rate constants differing from those for pH 7.2 are marked as bold text. The symbol # mean that for CYS – GABA and pH 8.0 fits with scenario Ib were unsuccessful.**

Scenario Ia		WT - GABA			WT – P4S			LEU - GABA			CYS - GABA		
pH		6.0	7.2	8.0	6.0	7.2	8.0	6.0	7.2	8.0	6.0	7.2	8.0
$k_{off}$	$ms^{-1}$	1.16											
$\delta_2$		4.03			0.16			2.2			0.27		
$\gamma_2$		<b>1.1</b>	4.46	<b>9</b>	<b>1.7</b>	4.46	<b>5</b>	<b>14</b>	20	<b>25</b>	<b>170</b>	195	<b>750</b>
$\beta_2$		16.5											
$\alpha_2$		1.69											
$d_2$		<b>7</b>	23.8	<b>36</b>	<b>9</b>	23.8	<b>26</b>	<b>22</b>	28.8	<b>45</b>	<b>22</b>	28.8	<b>180</b>
$r_2$		<b>0.17</b>	0.12	<b>0.09</b>	<b>0.15</b>	0.12		<b>0.24</b>	0.21	<b>0.18</b>	0.21		
Scenario Ib		WT - GABA			WT – P4S			LEU - GABA			CYS - GABA		
$k_{off}$	$ms^{-1}$	<b>0.2</b>	1.16	<b>4</b>	<b>0.05</b>	1.16	<b>3</b>	<b>0.6</b>	1.16	<b>1.9</b>	<b>0.4</b>	1.16	<b>&gt;100<sup>#</sup></b>
$\delta_2$		4.03			0.16			2.2			0.27		
$\gamma_2$		4.46						20			195		
$\beta_2$		16.5											
$\alpha_2$		1.69											
$d_2$		<b>7</b>	23.8	<b>36</b>	<b>5</b>	23.8	<b>25</b>	<b>21</b>	28.8	<b>43</b>	<b>5</b>	28.8	<b>&gt;675<sup>#</sup></b>
$r_2$		<b>0.17</b>	0.12		0.12			<b>0.25</b>	0.21	<b>0.18</b>	0.21		
Scenario II		WT - GABA			WT – P4S			LEU - GABA			CYS - GABA		
$k_{off}$	$ms^{-1}$	1.16											
$\delta_2$		4.03			0.16			2.2			0.27		
$\gamma_2$		4.46			<b>4.7</b>	4.46		<b>22</b>	20	<b>14</b>	<b>210</b>	195	<b>150</b>
$\beta_2$		<b>60</b>	16.5	<b>10</b>	<b>26.4</b>	16.5	<b>15</b>	<b>20</b>	16.5	<b>13</b>	<b>20</b>	16.5	<b>3.5</b>
$\alpha_2$		1.69			<b>0.9</b>	1.69		<b>1.2</b>	1.69	<b>2.5</b>	1.69		
$d_2$		23.8						28.8					
$r_2$		0.12						0.21					
Scenario III		WT - GABA			WT – P4S			LEU - GABA			CYS - GABA		
$k_{off}$	$ms^{-1}$	1.16											
$\delta_2$		4.03			0.16			2.2			0.27		
$\gamma_2$		4.46						20			195		
$\beta_2$		<b>55</b>	16.5	<b>12</b>	<b>50</b>	16.5	<b>15</b>	<b>25</b>	16.5	<b>14</b>	<b>20</b>	16.5	<b>5</b>
$\alpha_2$		1.69											
$d_2$		<b>21</b>	23.8	<b>25</b>	<b>21</b>	23.8		<b>28</b>	28.8	<b>35</b>	<b>25</b>	28.8	<b>50</b>
$r_2$		0.12						0.21					

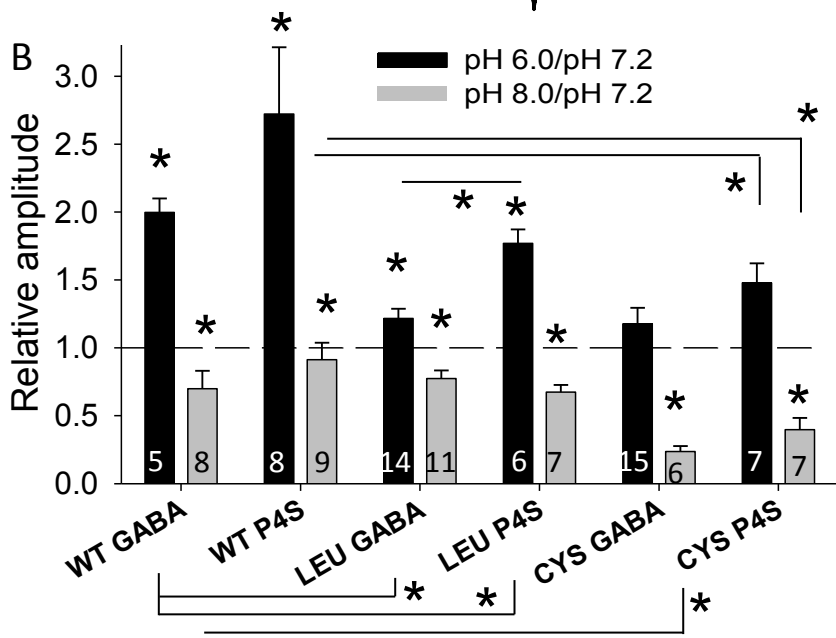
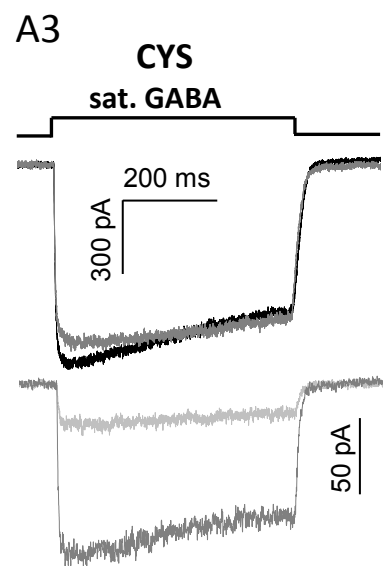
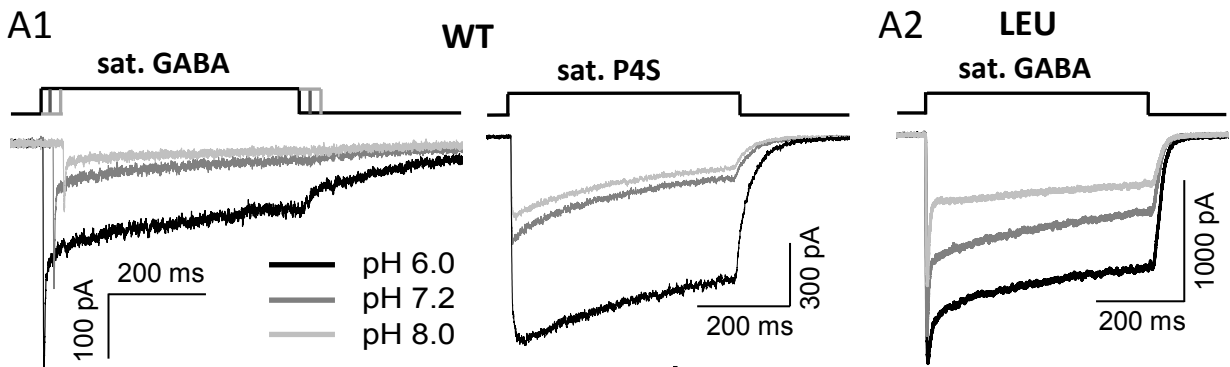
Table 2. Parameters of single-channel recordings ( $P$  – area,  $\tau$  – time constants of shut and open time distributions, burst duration and open probability calculated for clusters of bursts, bursts or for microbursts ( $t_{crit}$  between  $\tau_4 - \tau_5$ ,  $\tau_3 - \tau_4$  or  $\tau_2 - \tau_3$ , respectively). Time constants and areas (unbracketed values) were obtained from fitting experimental dwell time distributions for saturating [GABA] for wild-type  $\alpha_1\beta_2\gamma_2$  receptors at pH 7.4 and 6.0 with sums of exponentials. Time constants and areas in brackets represent values from distributions simulated with model 2 (Fig. 6B) which was optimized to the experimental data as described in Theory/calculation (normal brackets for experimental resolution and square brackets after correction for missed events). Data were expressed as the mean  $\pm$  SEM and calculated from 3-8 patches in each group. Bold text and \* mean  $p < 0.05$  for comparison to pH 7.4. The longest closures were not presented. Data for pH 7.4 are from (Kisiel et al., 2018).

Open times	$P_1$	$\tau_1$ [ms]	$P_2$	$\tau_2$ [ms]	$\tau_{open}$ [ms]	
pH 7.4	0.39 $\pm$ 0.06	1.61 $\pm$ 0.22	0.59 $\pm$ 0.06	5.15 $\pm$ 0.55	3.62 $\pm$ 0.32	
	(0.38 $\pm$ 0.07)	(0.86 $\pm$ 0.12)	(0.62 $\pm$ 0.07)	(5.36 $\pm$ 0.81)	(3.65 $\pm$ 0.35)	
	[0.67 $\pm$ 0.05]	[0.86 $\pm$ 0.12]	[0.33 $\pm$ 0.05]	[3.84 $\pm$ 0.83]	[1.67 $\pm$ 0.18]	
pH 6.0	0.55 $\pm$ 0.13	1.99 $\pm$ 0.20	0.45 $\pm$ 0.13	6.68 $\pm$ 0.66	4.05 $\pm$ 0.39	
	(0.53 $\pm$ 0.10)	(1.96 $\pm$ 0.19)	(0.47 $\pm$ 0.10)	(7.60 $\pm$ 0.43)	(4.09 $\pm$ 0.57)	
	[0.81 $\pm$ 0.03]	[1.07 $\pm$ 0.10]	[0.19 $\pm$ 0.03]	[4.59 $\pm$ 1.30]	[1.65 $\pm$ 0.22]	
Shut times	$P_1$	$\tau_1$ [ms]	$P_2$	$\tau_2$ [ms]	$P_3$	$\tau_3$ [ms]
pH 7.4	0.63 $\pm$ 0.04	0.06 $\pm$ 0.01	0.29 $\pm$ 0.04	0.30 $\pm$ 0.04	0.05 $\pm$ 0.01	2.27 $\pm$ 0.30
	(0.61 $\pm$ 0.04)	(0.07 $\pm$ 0.01)	(0.30 $\pm$ 0.03)	(0.31 $\pm$ 0.04)	(0.07 $\pm$ 0.02)	(2.11 $\pm$ 0.44)
	[0.66 $\pm$ 0.04]	[0.06 $\pm$ 0.01]	[0.26 $\pm$ 0.03]	[0.30 $\pm$ 0.04]	[0.05 $\pm$ 0.01]	[2.34 $\pm$ 0.43]
pH 6.0	0.65 $\pm$ 0.04	0.04 $\pm$ 0.003	0.18 $\pm$ 0.03	0.22 $\pm$ 0.03	<b>0.16<math>\pm</math>0.03*</b>	<b>1.15<math>\pm</math>0.17*</b>
	(0.66 $\pm$ 0.05)	<b>(0.04<math>\pm</math>0.002)*</b>	<b>(0.18<math>\pm</math>0.03)*</b>	(0.26 $\pm$ 0.03)	(0.15 $\pm$ 0.03)	(1.45 $\pm$ 0.36)
	[0.70 $\pm$ 0.05]	[0.04 $\pm$ 0.002]	[0.16 $\pm$ 0.03]	[0.26 $\pm$ 0.03]	<b>[0.13<math>\pm</math>0.03]*</b>	[1.44 $\pm$ 0.36]
pH	Burst duration [ms]	Open probability (in clusters)	Microburst duration [ms]	Open probability in microbursts		
7.4	198 $\pm$ 39 (58.5)	0.725 $\pm$ 0.035	56.6 $\pm$ 12.5 (17.6)	0.863 $\pm$ 0.010		
6.0	<b>380<math>\pm</math>56*</b> (148)	<b>0.839<math>\pm</math>0.025*</b>	<b>17.6<math>\pm</math>5.2*</b> (7.81)	<b>0.916<math>\pm</math>0.007*</b>		

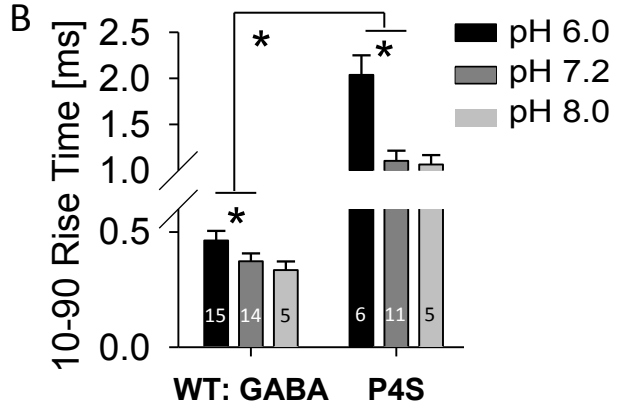
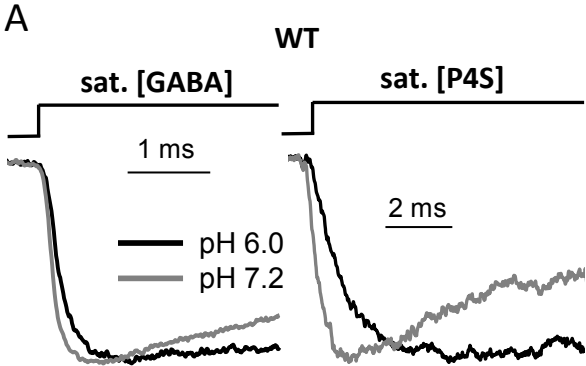
$p \leq 0.05$ : \* WT pH 6.0 vs. WT pH 7.4

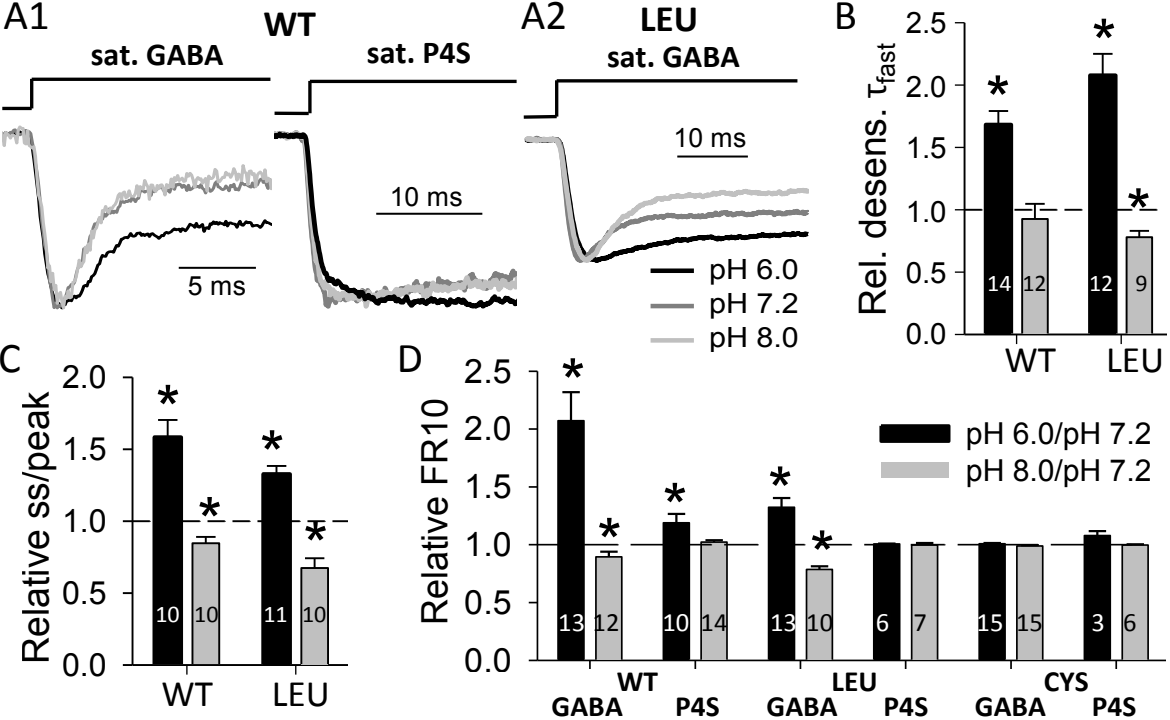
Table 3. Rate constants describing cluster kinetics evoked by saturating [GABA] for wild-type  $\alpha_1\beta_2\gamma_2$  GABA<sub>A</sub>Rs at pH 7.4 and 6.0. In simulations, the model with two doubly bound open states was used (Fig. 6B-D). Rate constants for pH 7.4 were previously presented in (Kisiel et al., 2018). The rate constants differing from those for pH 7.4 are marked as bold text (\*  $p \leq 0.05$ ). Desensitization rate constants describing relatively slow transitions ( $d_2$ ,  $r_2$ ,  $d_2'$ ,  $r_2'$  marked with grey colour), assessed in steady-state conditions, substantially differ from those assessed for macroscopic experiments using rapid solution exchange system.

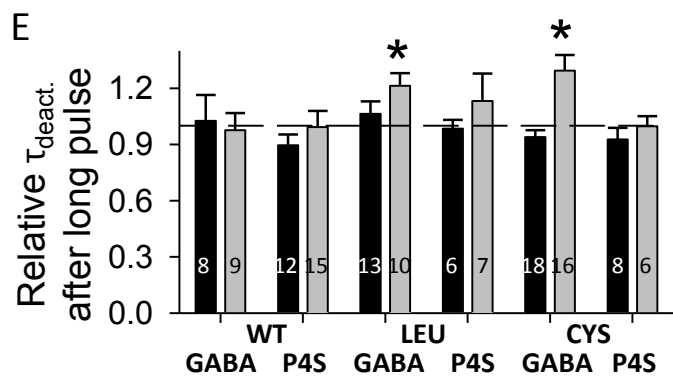
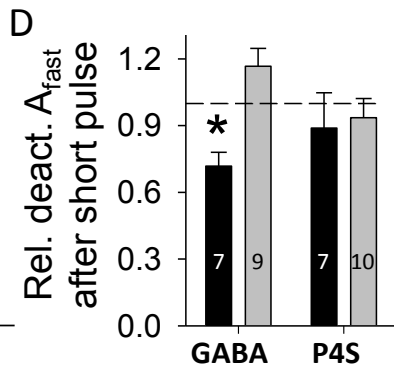
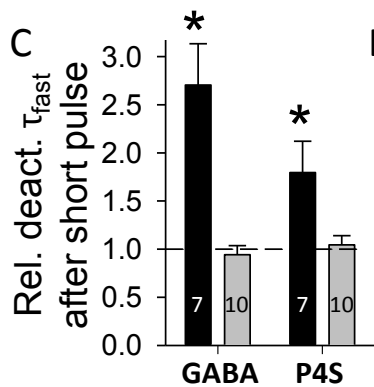
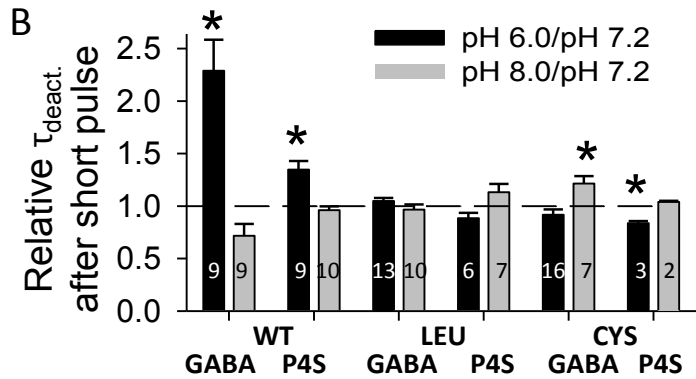
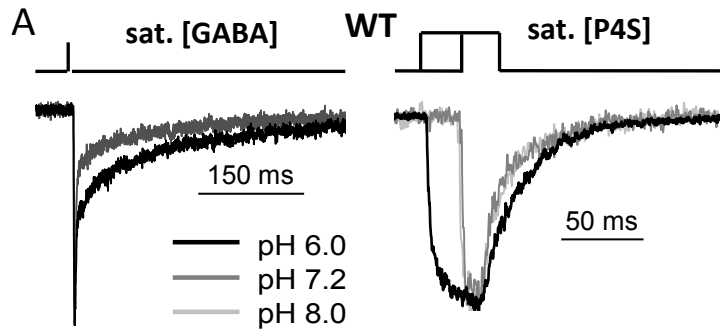
Rate constants [ $\text{ms}^{-1}$ ]	pH 7.4	pH 6.0
$\delta_2$	$5.07 \pm 0.81$	$4.83 \pm 0.64$
$\gamma_2$	$2.82 \pm 0.43$	$3.38 \pm 0.57$
$\alpha_2$	$1.35 \pm 0.20$	$0.96 \pm 0.09$
$\beta_2$	$9.29 \pm 1.62$	<b><math>15.36 \pm 1.70^*</math></b>
$\alpha_2'$	$0.33 \pm 0.05$	$0.36 \pm 0.18$
$\beta_2'$	$4.49 \pm 0.91$	$3.50 \pm 0.61$
$d_2$	$0.76 \pm 0.23$	<b><math>2.37 \pm 0.52^*</math></b>
$r_2$	$0.78 \pm 0.25$	$0.94 \pm 0.21$
$d_2'$	$0.28 \pm 0.12$	$0.16 \pm 0.06$
$r_2'$	$0.05 \pm 0.01$	$0.05 \pm 0.02$
resolution [ $\mu\text{s}$ ]	$66.0 \pm 1.6$	$60.0 \pm 4.1$

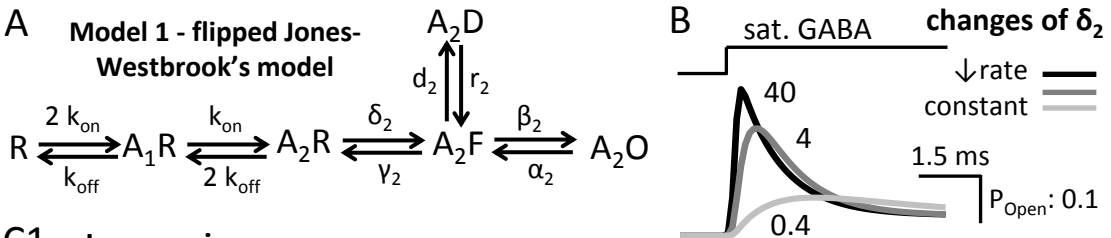




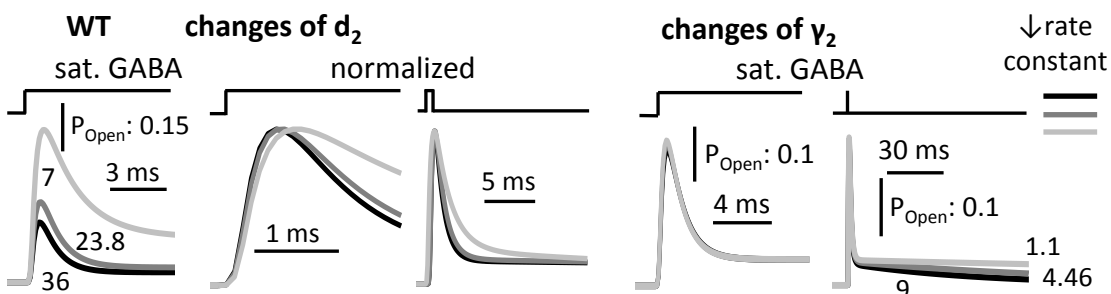




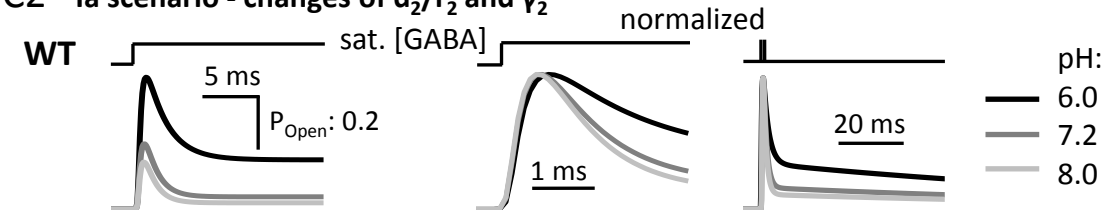




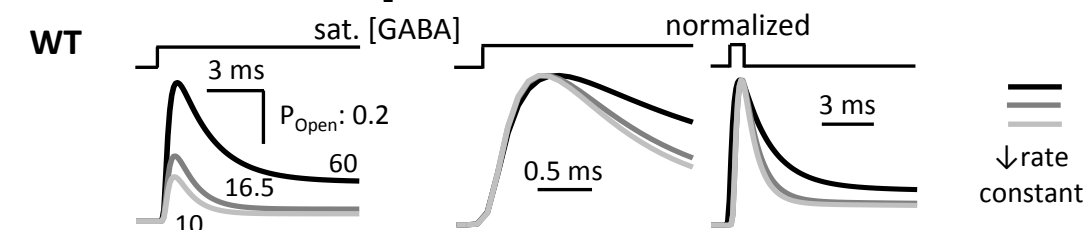
**C1 Ia scenario**



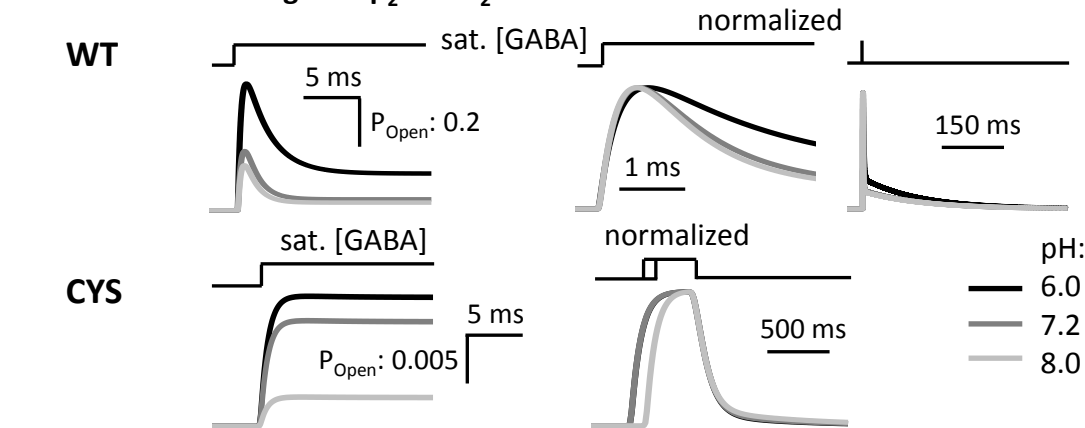
**C2 Ia scenario - changes of  $d_2/r_2$  and  $\nu_2$**

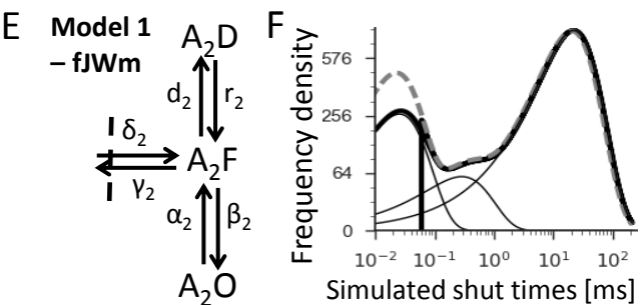
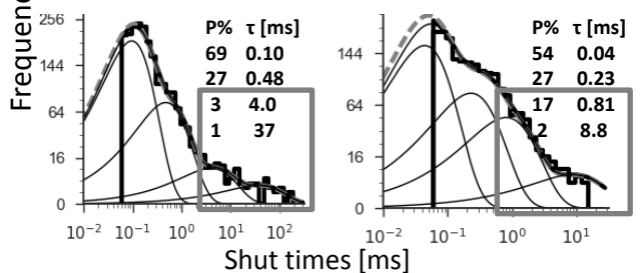
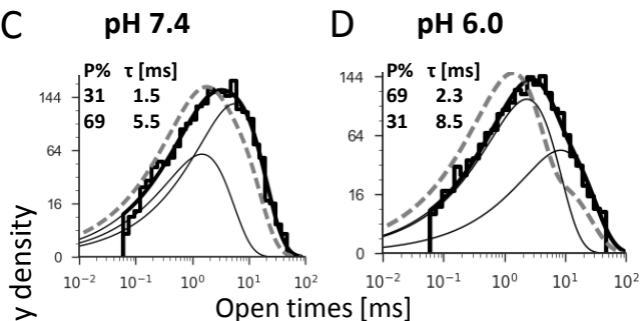
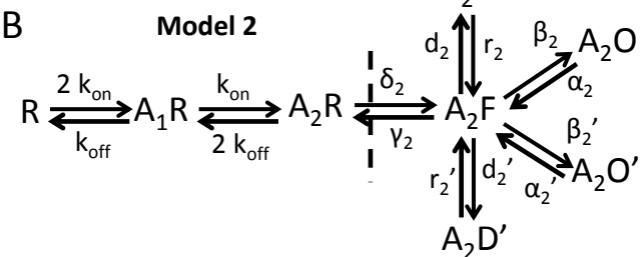
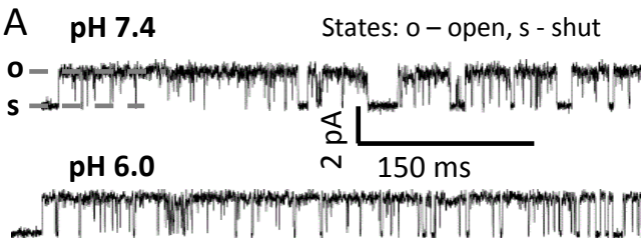


**D II scenario - changes of  $\beta_2$**



**E III scenario - changes of  $\beta_2$  and  $d_2$**





**Highlights**

- Extracellular pH changes affect open probability of GABA<sub>A</sub> receptor.
- Protons affect GABA<sub>A</sub>R by altering primarily desensitization and opening rates.
- Flipping transitions appear not to be affected by pH changes.
- $\alpha_1$ Phe64 mutations enhance receptor sensitivity to alkalization.